Taxonomic and Biochemical Characterization of Microalga *Graesiella emersonii* GEGS21 for Its Potential to Become Feedstock for Biofuels and Bioproducts

Nam Seon Kang [1] , Kichul Cho [1], Sung Min An [1], Eun Song Kim [1], Hyunji Ki [1], Chung Hyeon Lee [1], Grace Choi [1] and Ji Won Hong [2,3,*]

[1] Department of Microbial Resources, National Marine Biodiversity Institute of Korea, Seocheon 33662, Republic of Korea
[2] Department of Hydrogen and Renewable Energy, Kyungpook National University, Daegu 41566, Republic of Korea
[3] Advanced Bio-Resource Research Center, Kyungpook National University, Daegu 41566, Republic of Korea
[*] Correspondence: jwhong@knu.ac.kr; Tel.: +82-(0)53-950-4578; Fax: +82-(0)53-950-3889

Abstract: *Graesiella emersonii* is a commercially exploitable source of bioactive compounds and biofuels with potential applications in microalgae-based industries. Despite this, little taxonomical information is available. Therefore, proper identification and characterization are needed for the sustainable utilization of isolated microalgae. In this study, an axenically isolated unicellular green alga from the Geumgang Estuary, Korea was investigated for its morphological, molecular, and biochemical characteristics. The morphological characteristics were typical of *G. emersonii*. Molecular phylogenetic analysis of the 18S rDNA sequence verified that the isolate belonged to *G. emersonii* and was subsequently named *G. emersonii* GEGS21. It was isolated from brackish water, and its optimal growth temperature, salinity, and light intensity were at 28–32 °C, 0 M NaCl, and 130–160 μmol m^{-2} s^{-1}, respectively. The strain thrived over a range of temperatures (5–40 °C) and withstood up to 0.5 M NaCl. The isolate was rich in omega-6 linoleic acid (C$_{18:2}$ n-6, 26.3%) and palmitic acid (C$_{16:0}$, 27.5%). The fuel quality properties were determined, and biodiesel from GEGS21 could be used as a biodiesel blend. Value-added carotenoids lutein (1.5 mg g^{-1} dry cell weight, DCW) and neoxanthin (1.2 mg g^{-1} DCW) were biosynthesized as accessory pigments by this microalga. The biomass of this microalga may serve as feedstock for biodiesel production as well as producing valuable ω-6 and carotenoids.

Keywords: *Graesiella emersonii*; lutein; taxonomy; pigments; fatty acids; omega-6; biofuels; microalgae

1. Introduction

Microalgae are ubiquitous protists found in rivers, lakes, oceans, soils, and even extreme environments such as fresh or saltwater bodies with a low pH [1–6]. They are the primary producers in aquatic ecosystems and play crucial roles in global carbon and nutrient cycles, such as nitrogen and phosphorus cycles [7]. Due to their ability to convert carbon dioxide into a variety of useful organic compounds via photosynthesis [8–10], microalgae have recently attracted increasing attention. A number of studies have been conducted on the potential use of the microalgal biomass for bioenergy, nutraceutical, pharmaceutical, food, and cosmetic products, as well as agriculture and bioremediation applications [11–15]. Recently, the microalgae biorefinery concept has been proposed [16–19]. In this approach, microalgal biomass grown in wastewater can be converted into a range of bulk chemicals and value-added biocompounds [20]. Other technologies have also been integrated into microalgal biorefinery to facilitate the full-scale utilization of algal biomass [21,22].

Among green algae, Chlorophyta is one of the largest phyla with many species and a wide geographical distribution. Some can cause blooming in lentic systems during

the summer season under favorable conditions [23–25]. Additionally, several microalgal strains of Chlorophyta have been used as biotechnological resources [26–29]. However, *Chlorella*-like species have at times been misidentified because of their morphological simplicity [30]. Accurate species identification and delimitation have important implications for the safe consumption of commercial microalgal products [31–33]. Misidentified names of microalgae may potentially lead to economic losses and also pose a risk to public health [30]. Therefore, isolation and establishment of clonal cultures from a variety of environments are important steps to accurately identify species of interest. This will further our understanding of their potential commercial value.

The genus *Graesiella* was first established by Kalina and Puncochárová [34] and, to date, only one species (*Graesiella emersonii*) has been described in the genus [35]. *G. emersonii* is usually found in freshwater, but occasionally inhabits brackish water. As it is capable of water purification, *G. emersonii* plays an indispensable role in maintaining healthy aquatic ecosystems [36,37]. Moreover, *G. emersonii* is a promising resource for valuable pigments, lipids, and potential pharmaceuticals [38–41]. In addition, *G. emersonii* has been consumed in Europe and is an approved food supplement in France [42,43]. Furthermore, this species can be used to sustainably produce biodiesel during wastewater treatment [39]. Hence, *G. emersonii* is a commercially exploitable source of bioactive compounds and biofuels with potential applications in microalgae-based industries. However, despite their ecological and economic importance in marine ecosystems and biotechnology, not much information is available on their taxonomy because of the difficulties in culturing and observing their morphology using scanning electron microscopy (SEM) and transmission electron microscopy (TEM). Thus, their roles as essential components of aquatic ecosystems and their potential for biotechnology are often overlooked. Additionally, microalgal strains within the same species can exhibit different physiological activities and metabolite profiles [44,45]. It is expected that strains belonging to the same species but isolated from very different environments will demonstrate different physiological responses or exhibit different metabolite profiles. Hence, accurate identification followed by establishment of a clonal culture of this species is essential prior to further research and application.

In this study, we isolated a *G. emersonii* strain from brackish water in the Geumgang Estuary, Korea and characterized its morphological, molecular, and chemotaxonomic features.

2. Materials and Methods

2.1. Sample Collection and Isolation

Plankton samples from the brackish water were obtained from the Geumgang Estuary, Gunsan-si, Jeollabuk-do, Korea (36°0′8.2″ N, 126°45′10.8″ E) in May 2021, when the water temperature and practical salinity unit (PSU) were 18.4 °C and 21, respectively (Table 1 and Figure 1). The Geumgang Estuary has substantial variabilities in salinity as the freshwater is released irregularly and artificially from the coastal reservoir. To mimic eutrophication, the water sample was mixed with an equal volume of BG-11 medium (Sigma-Aldrich, St. Louis, MO, USA) and the mixture was allowed to stand for two days. Cultures were ascetically isolated using a streak plate technique on a 1.5% agar-containing BG-11 medium. The plates were incubated in a culture room at 28 °C under cool fluorescent light (~60 µmol m^{-2} s^{-1}) and a light/dark cycle of 14 h/10 h until green microalgal colonies formed. Single colonies were aseptically transferred to fresh BG-11 plates and this step was repeated until a pure culture was obtained. The axenic algal culture was confirmed by spreading 50 µL liquid culture of the single colony onto 1.5% Luria–Bertani (LB) agar plates, and was verified by 16S rRNA-based colony PCR. The isolated algal strain was maintained at 28 °C in a plant growth chamber (JSR, Gongju, Korea) with 150 rpm of shaking under continuous 60 µmol photons m^{-2} s^{-1} of cool-white, fluorescent illumination.

Table 1. Strain, location of collection (LC), water temperature (T, °C), salinity (S, PSU), and Gen-Bank accession number (GBAN) for rDNA sequences of *Graesiella emersonii* GEGS21 isolated from Geumgang Estuary, Gunsan-si, Jeollabuk-do, Korea.

Species	Strain	LC	Date	T (°C)	S (PSU)	Marker Gene	GBAN
G. emersonii	GEGS21	Geumgang Estuary	May 2021	18.4	21	SSU	OP592224
						ITS	OP592225
						LSU	OP592226
						*rbc*L	OP605746
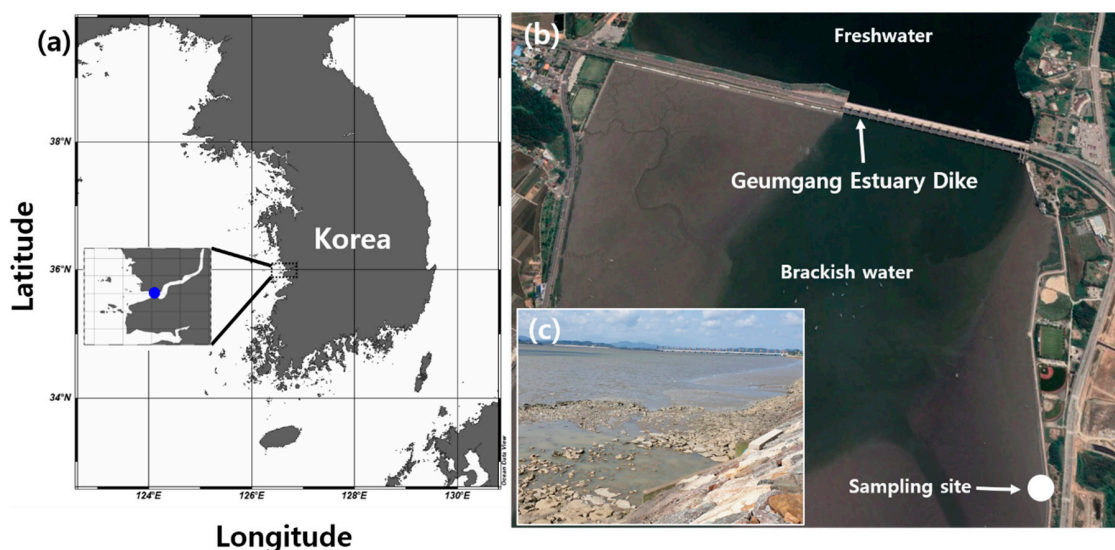
Figure 1. Location and photographs of the sampling site in the Geumgang Estuary, Korea. (**a**) Map of the sampling site; location of site in the Geumgang Estuary. The Geumgang Estuary is located at the mouth of the Geum River on the west coast of Korea. (**b**) The surrounding environment of the Geumgang Estuary in Korea; image acquired using Google Earth. (**c**) The image shows the sampling site of *Graesiella emersonii* GEGS21.

2.2. Morphological Identification

The morphology of living cells that had been grown photosynthetically was examined using an inverted microscope (CKX53, Olympus, Tokyo, Japan). The length and width of the live cells were measured using a digital camera (Zeiss AxioCam MRc5; Carl Zeiss, Göttingen, Germany). Additionally, to corroborate the location and presence of cell nuclei, samples were stained for 15 min with a nuclear marker (4′,6-diamidino-2-phenylindole, DAPI 10 μg mL^{-1} stock; Sigma-Aldrich) and analyzed using a UV filter under a fluorescence microscope (Zeiss Axio Imager 2; Carl Zeiss).

For field emission (FE)-SEM, 10 mL aliquots of cultures—at a density of approximately 2×10^6 cells mL^{-1}—were fixed for 10 min in osmium tetroxide (OsO$_4$, Electron Microscopy Sciences, Hatfield, PA, USA) at a final concentration of 1% (*v/v*). The fixed cells were collected on polycarbonate membrane filters which had 3 μm pores (Whatman Nuclepore Track-Etched Membranes; Whatman, Kent, UK) and were washed thrice with 50% filtered seawater diluted with distilled water to remove the residual salts. The membranes with attached cells were dehydrated in a graded ethanol series (10, 30, 50, 70, 90, and 100% ethanol), followed by two changes in 100% ethanol (Merck, Darmstadt, Germany), and were immediately dried using an automated critical point dryer (EM CPD300, Leica, Wetzlar, Germany). The dried filters were mounted on an aluminum stub (Electron Microscopy Sciences) using copper conductive double-sided tape (Ted Pella, Redding, CA, USA) and coated with gold using an ion sputter (MC1000, Hitachi, Tokyo, Japan). The cells and surface morphologies were observed using high-resolution Zeiss Sigma 500 VP FE-SEM (Carl Zeiss). For TEM, cells were transferred to a 10 mL tube and fixed in 2.5% (*v/v*)

glutaraldehyde (final concentration) for 1.5 h. The tube contents were placed in a 10 mL centrifuge tube and concentrated at $1610 \times g$ for 10 min in a centrifuge (VS-5500, Vision, Bucheon, Korea). The resulting pellet was subsequently transferred to a 1.5 mL tube and rinsed with 0.2 M sodium cacodylate buffer, pH 7.4 (Electron Microscopy Sciences). After several rinses with 0.2 M sodium cacodylate buffer, the cells were post-fixed for 90 min with 1% (w/v) OsO$_4$ prepared in deionized water. The pellet was embedded in agar. Dehydration was performed in a graded ethanol series (50, 60, 70, 80, 90, and 100% ethanol), followed by two changes in 100% ethanol. The material was then embedded in Spurr's resin (Electron Microscopy Sciences). Sections were prepared using an EM UC7 ultramicrotome (Leica, Wetzlar, Germany) and stained with 3% (w/v) aqueous uranyl acetate (Electron Microscopy Sciences), followed by 0.5% (w/v) lead citrate (Electron Microscopy Sciences). The sections were visualized using a Sigma 500/VP TEM (Carl Zeiss).

2.3. Molecular Identification

For molecular analysis, genomic DNA (gDNA) was extracted using an AccuPrep Genomic DNA Extraction Kit (Bioneer, Daejeon, Korea), as per the manufacturer's instructions. The rDNA was amplified using universal eukaryotic primers (Table 2). The reaction mixtures for PCR amplification comprised 5 µL of 10× F-Star Taq Reaction Buffer, 1 µL of 10 mM dNTP mix, 0.02 µM of primers, 0.25 µL of 5 U/µL BioFACT F-Star Taq DNA polymerase (BioFACT Co., Ltd., Daejeon, Korea), 38.75 µL of UltraPure DNAse/RNAse-Free Distilled Water (Invitrogen, Carlsbad, CA, USA), and 3 µL of the DNA template (ca. 10–30 ng DNA). PCR amplification was performed on an Eppendorf Mastercycler PCR machine (Eppendorf, Hamburg, Germany) under the following thermal cycling conditions: pre-denaturation at 94 °C for 5 min, followed by 40 cycles of 95 °C for 30 s, the selected annealing temperature (AT) for 30 s, 72 °C for 1 min, and a final extension at 72 °C for 10 min. The AT of the primers was determined by gradient PCR. We optimized the ATs as follows: 56 °C (EukA-G18R), 56 °C (570F-EukB), 57 °C (ITSF2-ITSFR2), 57 °C (D1R-LSUB), and 57 °C (*rbc*L-192-*rbc*L-657). PCR products were purified using the AccuPrep PCR Purification Kit (Bioneer) and subjected to Sanger sequencing (Macrogen, Daejeon, Korea). Nucleotide sequences were identified using NCBI BLAST. Alignments and phylogenetic and molecular evolutionary analyses of the small subunit (SSU) rDNA sequences were performed using Geneious Prime v.2022.2.2 (Biomatters Ltd., Auckland, New Zealand), with diverse assemblages using other species data available in NCBI GenBank. Bayesian analyses were run using MrBayes v.3.2.7 [46,47] with the default GTR + G + I model to determine the best available model for the data of each region. For all sequence regions, four independent Markov chain Monte Carlo runs were performed, as described by Kang et al. [48]. Maximum-likelihood (ML) analyses were conducted using RAxML v.8.2.10 [49]. Two hundred independent free inferences were allowed and the–# option was used to identify the best tree. Bootstrap values (MLBS) were calculated with 1000 replicates using the same substitution model.

Table 2. Primers used in this study to amplify the SSU, ITS, LSU region of rDNA, and the *rbc*L genes of *Graesiella emersonii* GEGS21.

Primer Name	Primer Region	Sequence (5′-3′)	References
EukA	Forward, SSU	AACCTGGTTGATCCTGCCAG	[50]
G18R	Reverse, SSU	GCATCACAGACCTGTTATTG	[51]
570F	Forward, SSU	GTAATTCCAGCTCCAATAGC	[52]
EukB	Reverse, SSU	TGATCCTTCTGCAGGTTCACCTAC	[50]
ITSF2	Forward, ITS	TACGTCCCTGCCCTTTGTAC	[51]
ITSFR2	Reverse, ITS	TCCCTGTTCATTCGCCATTAC	[51]
D1R	Forward, LSU	ACCCGCTGAATTTAAGCATA	[53]
LSUB	Reverse, LSU	ACGAACGATTTGCACGTCAG	[51]
*rbc*L-192	Forward, *rbc*L	GGTACTTGGACAACWGTWTGGAC	[54]
*rbc*L-657	Reverse, *rbc*L	GAAACGGTCTCKCCARCGCAT	[54]

2.4. Determination of Optimal Culture Conditions

Routine serial sub-culturing on the BG-11 agar slant was performed to maintain a pure culture of *G. emersonii*. A single colony of GEGS21 was streaked onto BG-11 agar plates containing glucose (1.0 g L^{-1}) as the sole carbon source in triplicate and incubated for 21 days. Finally, a single colony was cultured in BG-11 medium, and a subsequent optimal culture test was conducted at a laboratory scale. Optimal salinity was determined using a daily growth test at 28 °C with BG-11 media at NaCl concentrations of 0, 0.5, 1.0, 1.5, and 2.0 M for 10 days in a shaking incubator (JSR). Daily growth was analyzed using a DHC-N01 hemocytometer (INCYTO, Cheonan, Korea). Furthermore, optimal temperature and illumination analyses were conducted simultaneously using a PhotoBiobox [55]. Briefly, a 200 µL algal culture aliquot was injected into 96-well black/clear bottle plates and covered using a well plate sealing film. After incubation for 72 h in PhotoBiobox controlled at 5–40 °C of temperature, and 0–300 µmol m^{-2} s^{-1} of illumination, 600 nm of absorbance was analyzed using a Synergy II microplate reader (Biotek, Winooski, VT, USA). Specific growth rate was determined, and a heat map was generated using R 4.2.1 (The R Project for Statistical Computing, https://www.r-project.org, accessed on 16 October 2022).

2.5. Analyses for Fatty Acid Composition of Lipids and Their Biodiesel Properties

Lipid extraction was performed using a modification of the Blight–Dyer method developed by Breuer et al. [56]. The fatty acid methyl ester (FAME) composition was analyzed using a 7890A gas chromatograph equipped with a 5975C mass selective detector (Agilent, Santa Clara, CA, USA), in accordance with the methodology used in our previous study [57]. Compound identification was performed by matching the mass spectra with those in the Wiley/NBS registry of the mass spectral data. A search with a match value greater than 90% was considered valid. Biodiesel properties, including saponification value (SV), iodine value (IV), degree of unsaturation (DU), monounsaturated fatty acid (MUFA), polyunsaturated fatty acid (PUFA), long-chain saturation factor (LCSF), cold filter plugging point (CFPP), cetane number (CN), and oxidative stability (OS), based on the FAME profiles were calculated in accordance with the method described by Islam et al. [58].

2.6. Microalgal Pigment Extraction and Analysis

Algal photosynthetic pigment extraction was performed using the method described by Baek et al. [59] with slight modifications. Briefly, 1 mg freeze-dried biomass was extracted using 90% HPLC-grade acetone (Daejung, Siheung, Korea) and filtered through a Whatman polytetrafluoroethylene (PTFE) syringe filter with a pore size of 0.2 µm (Whatman, Florham Park, NJ, USA). Samples were then analyzed on an Agilent 1260 Infinity HPLC system (Agilent, Waldbronn, Germany) equipped with a Spherisorb 5.0 µm ODS1 4.6 × 250 mm cartridge column (Waters, St. Louis, MO, USA) at 33 °C. Pigment profiles were detected and quantified based on absorbance at 445 and 670 nm using a diode array detector. The mobile-phase gradient was programmed as described by Baek et al. [59] at a constant flow rate of 1.2 mL min^{-1} using a mixture of 2% methanol, 14% 0.1 M Tris-HCl (pH 8.0), and 84% acetonitrile (Solvent A, *v/v*) from 0 to 15 min, and a mixture of 32% acetonitrile 68% methanol (Solvent B, *v/v*) from 15 to 19 min, and the post-run was performed for 6 min using a Solvent A. The concentration of each pigment was analyzed using the HPLC profile determined using chlorophyll and carotenoid standard solutions (DHI, Hørsholm, Denmark).

3. Results

3.1. Morphology or Morphological Characteristics

The single vegetative cells of *G. emersonii* GEGS21 in culture were nearly spherical to ellipsoidal in shape (Figure 2a,b). The cells exhibited variable sizes but were most commonly 8.8–14.4 µm (12 ± 0.3, n = 20) in diameter (Table 3). A cup-shaped chloroplast

was observed along the cell periphery (Figure 2a), and a single pyrenoid was clearly visible in the vegetative cells as well as in the reproductive cells (Figure 2a,c). A single nucleus was located next to the pyrenoid (Figure 2a,b) and several nuclei (Figure 2b,c, Table 3) were observed in mature cells. Actively growing cultures showed asexual reproduction via autosporulation (Figure 2c–f). Parental and daughter cells were observed in all cultures examined by light microscopy, and most parental cells contained two, four, or six daughter cells (Figure 2c–f), but eight or more daughter cells were also observed (not shown). The daughter cells in the parental cell were globose or spheroidal to ellipsoidal (Figure 2g) and were 5.0–12.7 μm (6.9 ± 0.4, n = 20) in diameter (Table 3). The daughter cells with chloroplasts, nuclei, and prominent pyrenoids were released through parental cell wall rupture (Figure 2g).
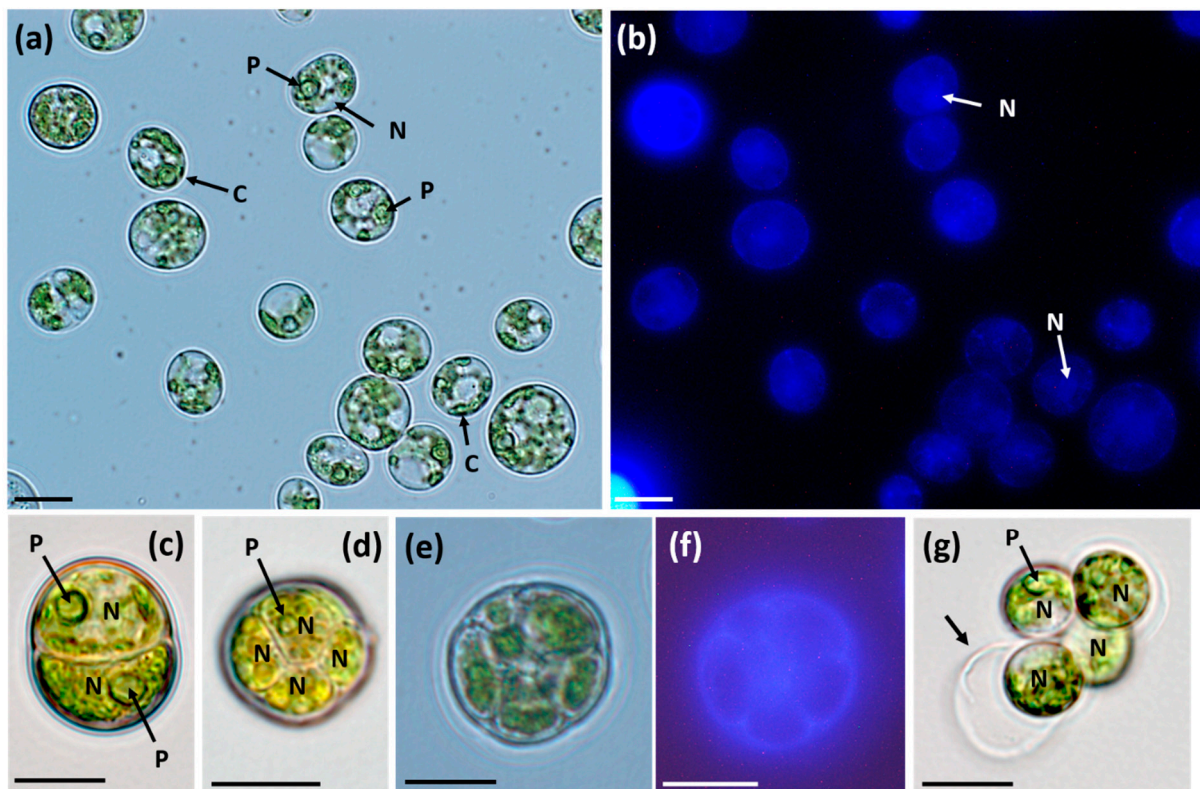
Figure 2. Light and epifluorescence micrographs of the vegetative and reproductive cells from *Graesiella emersonii* GEGS21. (**a**) Vegetative cells are green, unicellular, and grow in variable forms from spheroidal to ellipsoidal. A single pyrenoid (P), nucleus (N), and cup-shaped chloroplast (C) is visible. (**b**) Uninuclear cells were stained with DAPI and observed under fluorescence. The arrow indicates the nucleus (N). (**c,d**) Vegetative cells in different stages of development, autospores. Micrographs showing a nucleus (N) and pyrenoid (P). (**e,f**) Light (**e**) and epifluorescence (**f**) micrographs of several daughter protoplasts are formed in the parental cell wall. (**g**) Light micrograph of daughter cells released from the parental cell. The arrow indicates the ruptured parental cell wall. Micrographs showing a nucleus (N) and pyrenoid (P). Scale bars: (**a–g**) = 10 μm.

Table 3. Comparison of morphological and ultrastructural characteristics among *Graesiella emersonii* strains.

| Character Traits	GEGS21	NIES-226	Maryland Culture Collection No. 2	CCAP211/11N
Strain locality	Korea	Japan	USA	Germany
Cell shape	Spherical to ellipsoidal	Spherical	Spherical or ellipsoidal	Spherical
Cell size (μm; vegetative cells)	8.79–14.4 (11.6)	~17	4–16	3–17
Cell size (μm; daughter cells)	5.0–12.7 (6.9)	5.4–7.1 (5.9) *	ND	ND
Pyrenoid	Present, surrounded by the starch grains	Present, surrounded by the starch grains	Present	Present, surrounded by the starch grains
Numbers of nuclei (mature cell)	More than two nuclei, sometimes remained single	More than two nuclei, sometimes remained single	ND	More than two nuclei, sometimes remained single
Numbers of daughter cells (in parental cell)	2, 4, 8, or 16	4, 8, or 16	ND	2, 4, 8, or 16
Vacuoles	Numerous	Numerous	ND	ND
Cell wall	Composed of a trilaminar sheath and fibrillar wall	Composed of a trilaminar sheath	ND	Composed of a trilaminar sheath
Cell wall ribs	Most cells have meridional or irregular network ribs	Lacking meridional ribs, but sometimes developing minute ribs	ND	ND
References	This study	[60]	[61]	[60,62]

ND, information not available; * Not mentioned, but measured from figures. Mean values are shown in parentheses.

Scanning electron micrographs of a group of vegetative and reproductive cells of *G. emersonii* GEGS21 are shown in Figures 3 and 4. Figure 3a shows an example of variable forms, from globose to ellipsoidal cells, which were found in variable sizes. As shown in the micrographs, the parental and daughter cells exhibited characteristic cell wall sculptures in the form of a meridional or irregular network of fine ribs (Figure 4a–e). The number of fine ribs varied according to various stages of development of the parental and daughter cells (Figure 4a–e). Scanning electron micrographs showed that the parental cell wall was composed of multiple layers (Figure 4f,g).

Transmission electron micrographs of the vegetative and reproductive cells of *G. emersonii* GEGS21 are shown in Figure 5. Figure 5a shows an example of variable forms, from globose to ellipsoidal cells, which were found in variable sizes. Chloroplasts were observed along the cell periphery (Figure 5a–c). The pyrenoid matrix was surrounded by starch grains and was present in the chloroplasts (Figure 5b). The thylakoids that surround the pyrenoid never directly touched the surface of the pyrenoid and did not penetrate it (Figure 5b). A single nucleus was located adjacent to the pyrenoid (Figure 5b). Two nuclei were frequently observed in mature cells (Figure 5c); however, the occurrence of multiple nuclei per cell was also seen (not pictured). Some cells and electron-dense bodies (DB) were observed (Figure 5d). Thin TEM sections showed the structure of the *G. emersonii* GEGS21 cell wall, which was composed of a trilaminar sheath (TLS) and fibrillar wall (Figure 5f). The TLS appeared as a translucent line inserted between two electron-dense lines. The fibrillar wall was located between the TLS and plasma membrane (Figure 5f). Overall, the strain GEGS21 exhibited the typical morphology of *G. emersonii*.
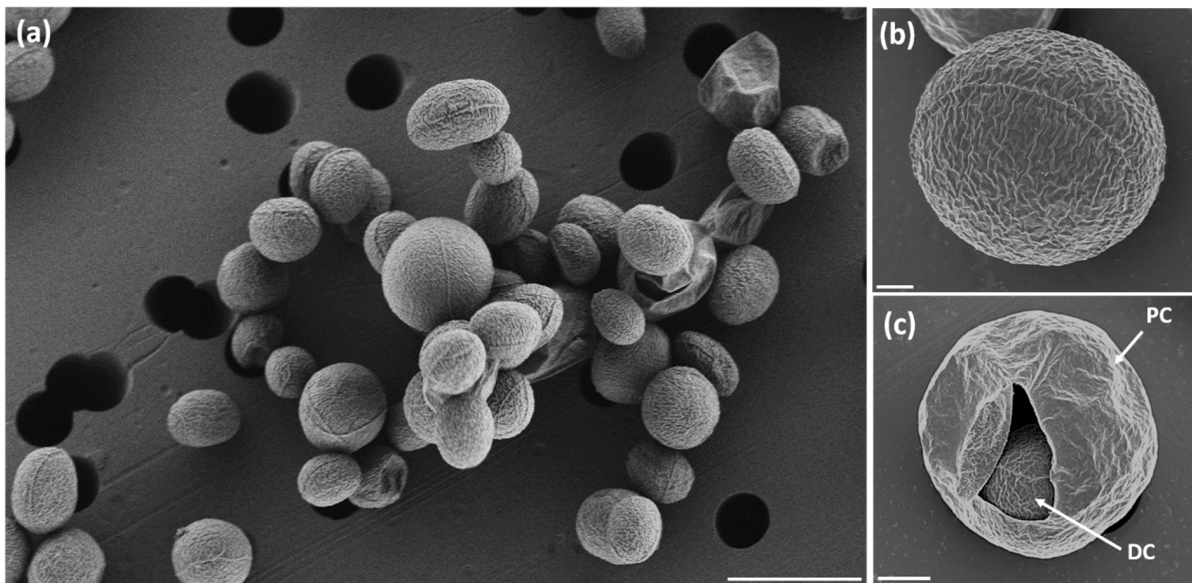
Figure 3. Scanning electron micrographs of the strain *Graesiella emersonii* GEGS21 cells. (**a**) Various shapes and sizes of *G. emersonii* GEGS21. (**b**) Vegetative cell. (**c**) Parental cell (PC) and daughter cell (DC). Scale bars: (**a**) = 10 μm, (**c**) = 2 μm, (**b**) = 1 μm.
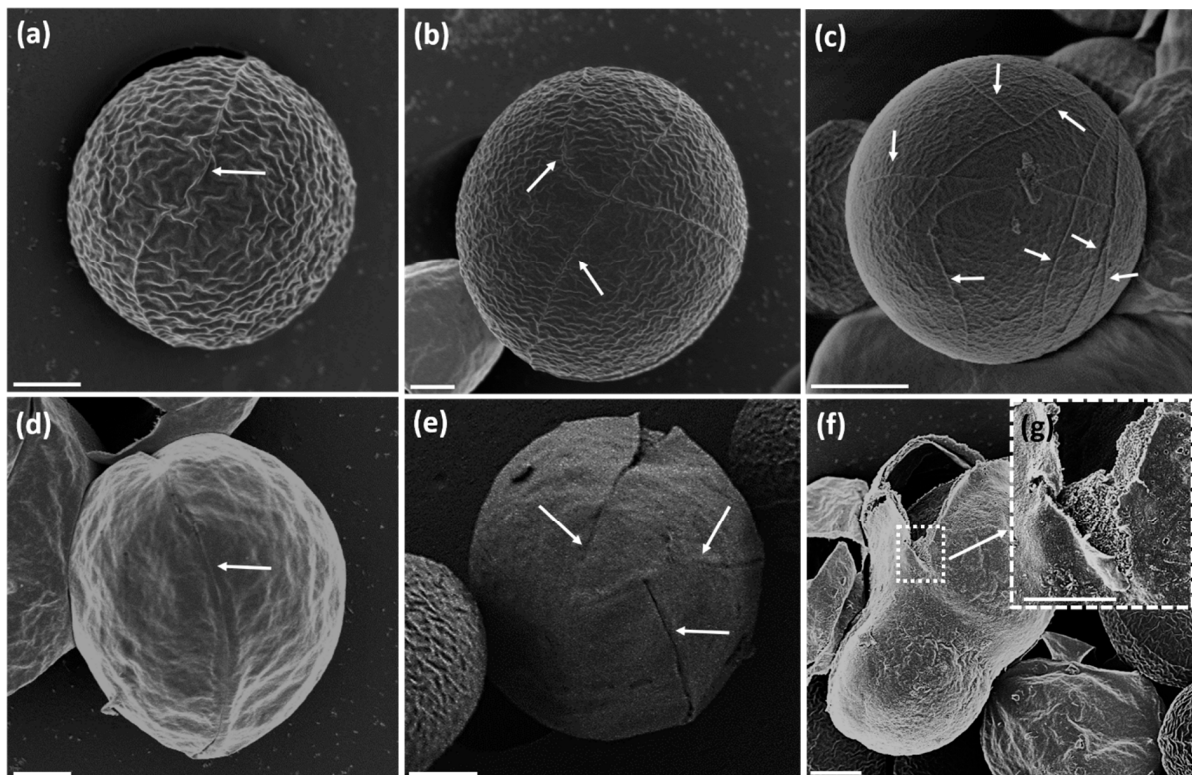
Figure 4. Scanning electron micrographs of the strain *Graesiella emersonii* GEGS21 cells. (**a**–**c**) Vegetative cell with fine ribs on the surface. The arrow indicates the fine ribs. (**d**,**e**) Parental cell with fine ribs on the surface. The arrow indicates the fine ribs. (**f**) SEM of the ruptured parental cell wall. (**g**) Enlarged SEM of (**f**), showing the outer layer of the parental cell wall. Scale bars: (**c**) = 3 μm, (**f**) = 2 μm, (**a**,**b**,**d**,**e**,**g**) = 1 μm.
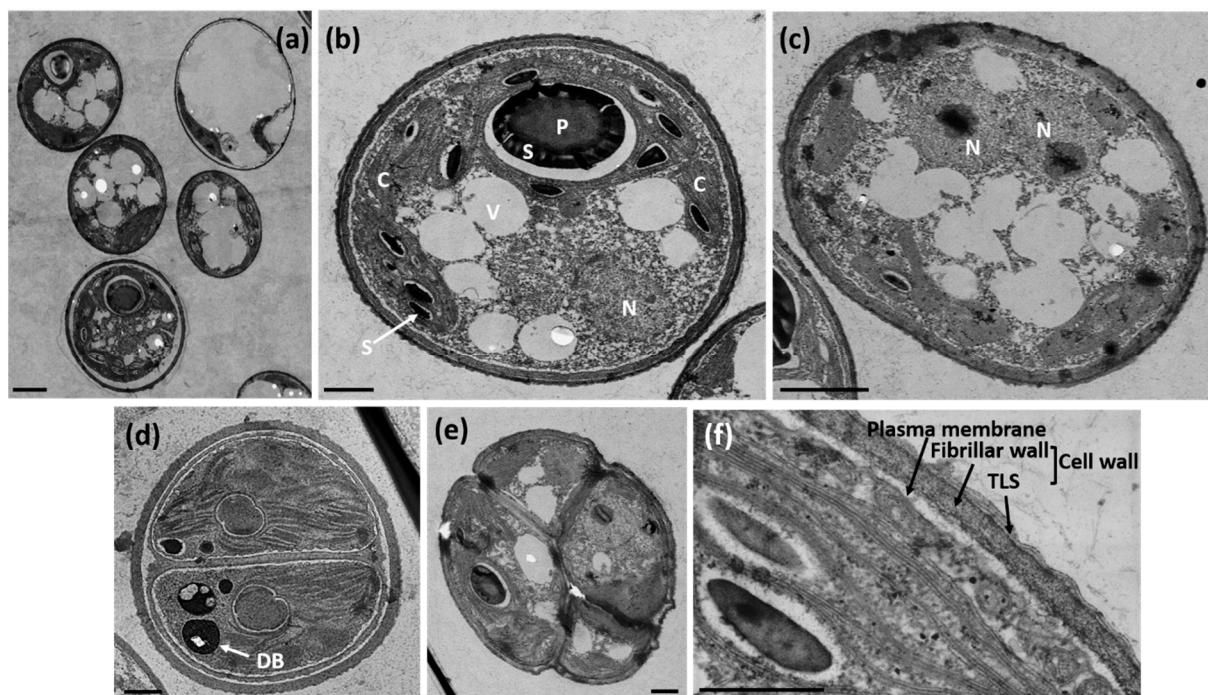
Figure 5. Transmission electron micrographs of *Graesiella emersonii* GEGS21 cells. (**a**) Various shapes and sizes of *G. emersonii* GEGS21. (**b**) Micrograph showing a chloroplast (C), nucleus (N), pyrenoid (P), starch (S), and vacuoles (V). (**c**) TEM of vegetative cell showing two nuclei (N). (**d**,**e**) TEM showing the formation of autospores, two (panel **d**) and four (panel **e**) cells are visible. DB; electron-dense body. (**f**) TEM micrograph of cell wall structure shows two main layers: trilaminar sheath (TLS) and fibrillar wall. The plasma membrane is also visible. Scale bars: (**a**,**c**) = 2 μm, (**b**,**d**,**e**) = 1 μm, (**f**) = 0.5 μm.

3.2. Molecular Identification and Sequence Analysis

The SSU, ITS1, 5.8S, ITS2, and LSU rDNA sequences and *rbc*L genes (GenBank accession no. OP592224–OP592226, OP605746; Table 1) of the new isolate comprised 3139 nucleotides. When properly aligned, the sequence of SSU rDNA of *G. emersonii* GEGS21 was identical to that of *G. emersonii* strains CCAP 211/11N (Berlin, Germany), BEA0616B (Gran Canaria, Spain), BEA1005B (Cadiz, Spain), NT1e (Tennant Creek, Australia), CCAP 211/15 (England), CCAP 211/11M (unknown), CCAP 211/8H (unknown), and CCAP 211/8P (unknown), while *G. emersonii* strains NIES-2151 (Berlin-Dahlem, Germany), NIES-690 (Berlin, Germany), and unknown Indian strains have a 1–8 base substitution in the SSU compared to strain GEGS21 (Table 4). In the phylogenetic tree based on SSU rDNA sequences, *G. emersonii* GEGS21 formed a large clade (i.e., *Graesiella emersonii*) with strains NIES-2151, CCAP211/15, NIES-690, BEA1005B, BEA0616B, NT1E, CCAP211/8H, CCAP211/11N, CCAP211/11M, CCAP211/8P, and unknown strains (GenBank accession no. KJ725233 and MN877773) (Figure 6). Molecular characterization inferred from sequence analyses of SSU rDNA showed that the isolate was a member of the *G. emersonii* group (Table 4, Figure 6). Therefore, this microalga was identified as *G. emersonii* GEGS21 and deposited at the National Marine Biodiversity Institute of Korea (MABIK) and the Korean Collection for Type Cultures under the accession numbers MABIK LP00000155 and KCTC15115BP, respectively.
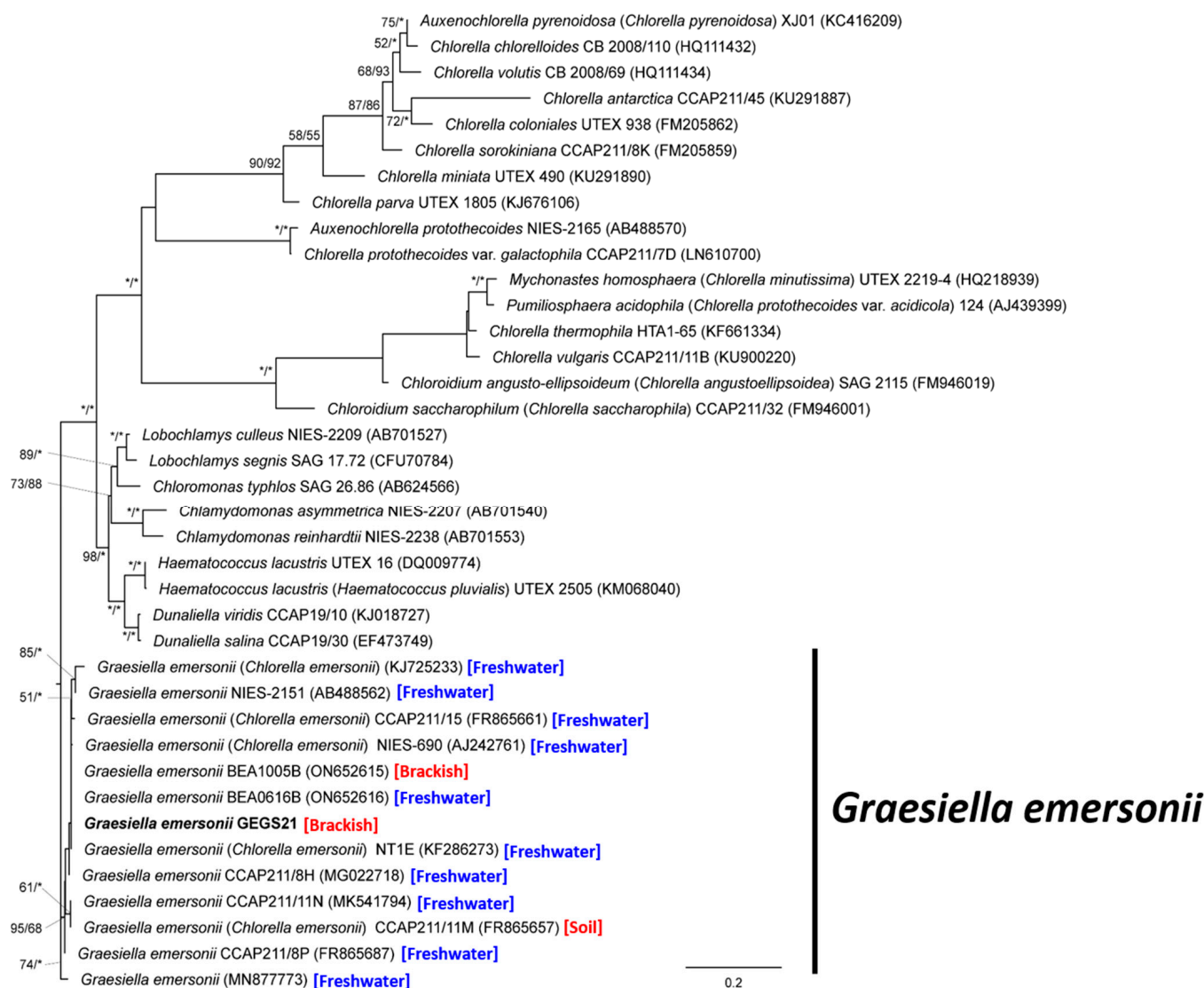
Figure 6. Maximum-likelihood and Bayesian inference phylogenetic tree based on the 18S rDNA sequence. The values on each node indicate maximum-likelihood bootstrap and Bayesian posterior probabilities (%), respectively. Bootstrap values lower than 50 and Bayesian posterior probabilities lower than 75 are not shown. * = 100. Our strain is shown in bold.

Table 4. Comparison of small subunit rDNA sequence of *Graesiella emersonii* GEGS21 isolated from the Geumgang Estuary of Korea and other strains.

Collection Location	Strain Habitat (Isolation Source)	Strain Name	GenBank Accession No.	*Graesiella emersonii* GEGS21 *
Berlin, Germany	Freshwater	CCAP 211/11N	MK541794	0 (0)
Gran Canaria, Spain	Freshwater	BEA0616B	ON652616	0 (0)
Cadiz, Spain	Brackish	BEA1005B	ON652615	0 (0)
Tennant Creek, Australia	Freshwater	NT1e	KF286273	0 (0)
England	Freshwater	CCAP 211/15	FR865661	0 (0)
ND	Soil	CCAP 211/11M	FR865657	0 (0)
ND	Freshwater	CCAP 211/8H	MG022718	0 (0)
ND	Freshwater	CCAP 211/8P	FR865687	0 (0)
Berlin-Dahlem, Germany	Freshwater	NIES-2151	AB488562	2 (0.1)

Table 4. *Cont.*

Collection Location	Strain Habitat (Isolation Source)	Strain Name	GenBank Accession No.	*Graesiella emersonii* GEGS21 *
Berlin, Germany	Freshwater	NIES-690	AJ242761	1 (0.2)
India	Freshwater	ND	MN877773	8 (0.9)
Mumbai, India	Freshwater	ND	KJ725233	7 (1.3)

* The numbers indicate the number of base pairs that differ from *G. emersonii* GEGS21. The numbers in parentheses indicate dissimilarity (%), including gaps. ND, information not available.

3.3. Verification of the Optimal Cultivation Conditions of the Isolated Strain

To verify the optimal cultivation conditions for the isolated algal strain, growth responses to different salinities, temperatures, and light intensities were determined under laboratory-scale conditions. As shown in Figure 7, a salinity-dependent decrease in the daily growth of *G. emersonii* was observed after 10 days of cultivation. Specifically, the exponential growth phase appeared after 3 days, and approximately 3.1×10^6 cells mL^{-1} were counted at a 0.5 M NaCl concentration. However, approximately 5.48-fold higher cell numbers (1.7×10^7 cells mL^{-1}) were counted at 0 M NaCl after 10 days, and no growth was observed at an NaCl concentration of 1.0–2.0 M. As shown in Figure 8, *G. emersonii* GEGS21 grew at temperatures between 5 and 40 °C, and the highest growth rate was determined at 28–32 °C and 130–160 μmol m^{-2} s^{-1} of light intensity (white LED). In conclusion, the strain thrived over a wide range of temperatures (5–40 °C) and withstood up to 0.5 M NaCl.
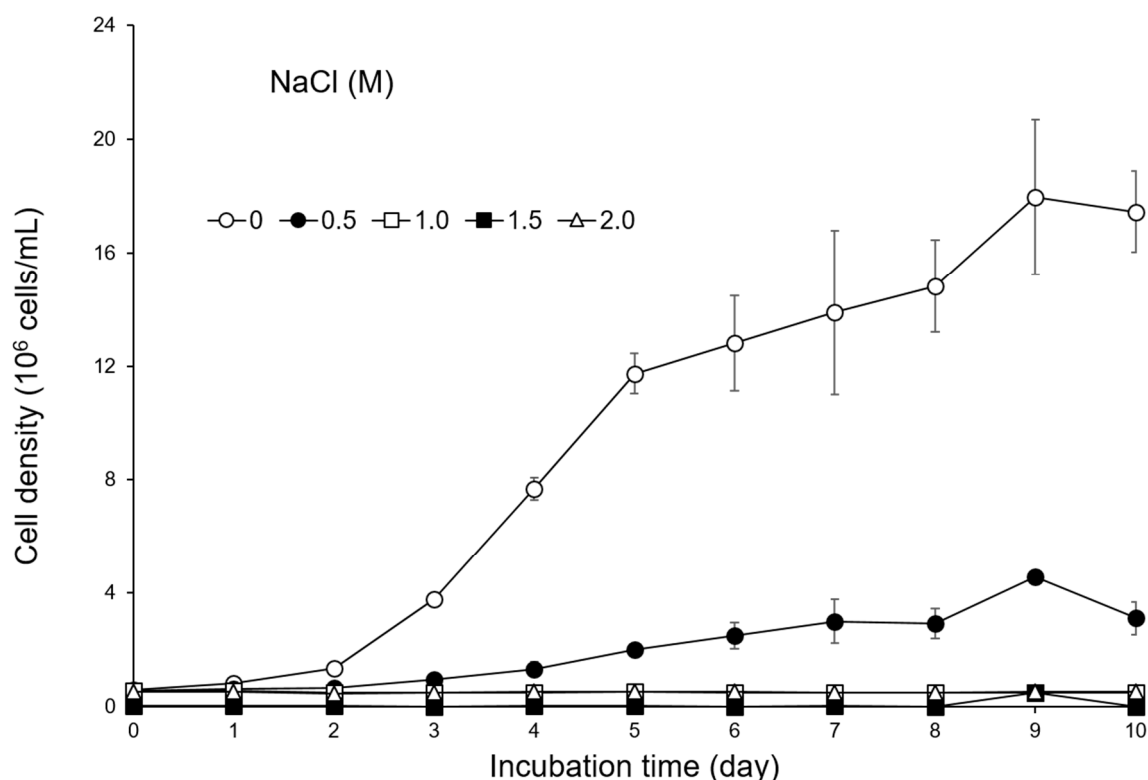
Figure 7. Effect of salt (NaCl, M) supplementation on the density of *Graesiella emersonii* GEGS21.
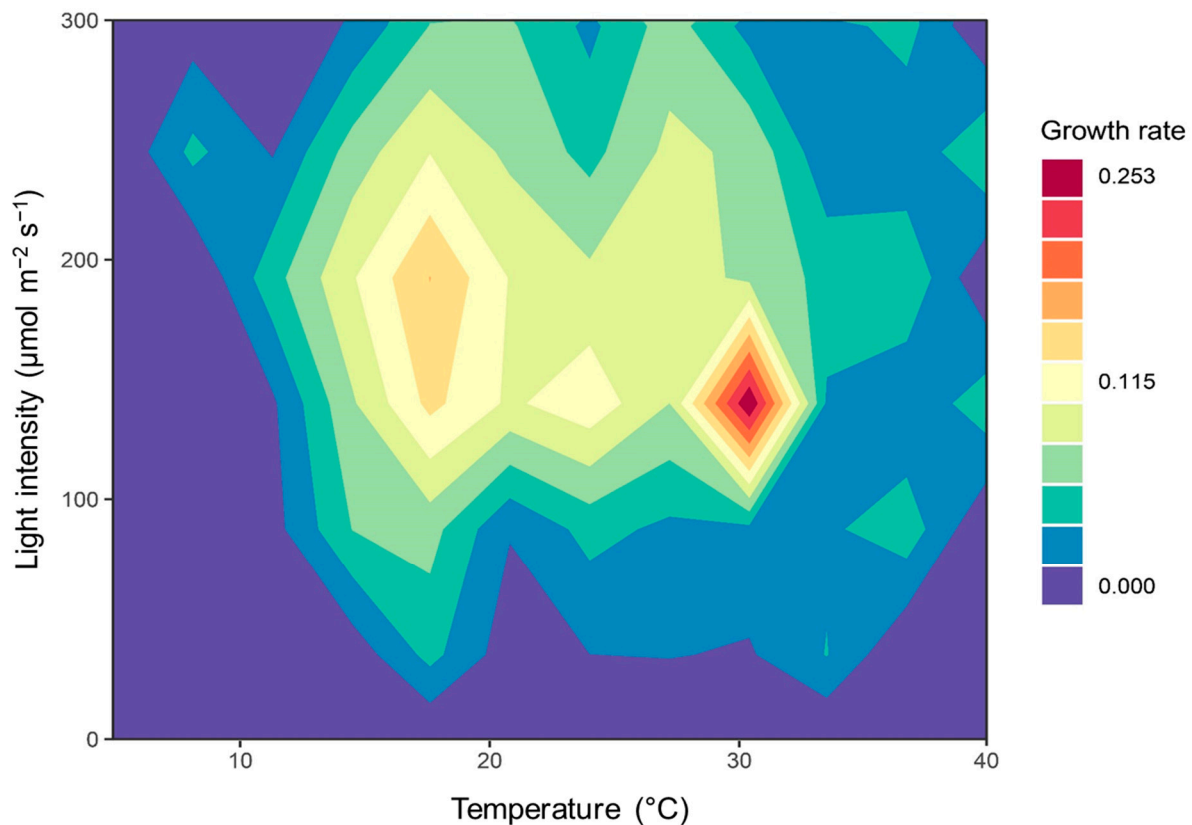
Figure 8. Matrix of growth rate (as shown in the legend) under different temperature and light regimes for *Graesiella emersonii* GEGS21.

3.4. Fatty Acid Composition of Lipids and Their Biodiesel Properties

Gas chromatography/mass spectroscopy (GC/MS) analysis revealed the FAME profiles of *G. emersonii* GEGS21 (Table 5). The major FAME profiles of *G. emersonii* GEGS21 were $C_{16:0}$ (27.5%), $C_{18:1}$ n-9 (22.2%), $C_{18:2}$ n-6 (26.3%), and $C_{18:3}$ n-3 (22.1%) (Table 5). In addition, trace amounts of saturated fatty acids (SFAs, $C_{18:0}$, 0.6%), polyunsaturated fatty acids (PUFAs, $C_{18:3}$ n-6, 1.0%), and monounsaturated fatty acids (MUFAs, $C_{20:1}$ n-9, 0.3%) were also detected (Table 5). Eicosapentaenoic acid (EPA, $C_{20:5}$ n-3) and docosahexaenoic acid (DHA, $C_{22:6}$ n-3) were not detected in the strain GEGS21 (Table 6).

Table 5. Lipid profile of *Graesiella emersonii* strain GEGS21.

Component	Content (%)	Note
Palmitic acid ($C_{16:0}$)	27.5	SFA (major)
Stearic acid ($C_{18:0}$)	0.6	-
Oleic acid ($C_{18:1}$ n-9)	22.2	Omega-9 MUFA (major)
Linoleic acid ($C_{18:2}$ n-6)	26.3	Omega-6 PUFA (major)
g-linolenic acid ($C_{18:3}$ n-6)	1.0	-
α-linolenic acid ($C_{18:3}$ n-3)	22.1	Omega-3 PUFA (major)
Eicosenoic acid ($C_{20:1}$ n-9)	0.3	-

Table 6. Fatty acid percentage comparisons of *Graesiella emersonii* strains, other microalgae, and selected second-generation oil sources. BACI, bacillariophyte (diatom); BIG, bigyra; CHL, chlorophyte; DHA, docosahexaenoic acid; DINO, dinoflagellate; DPA, docosapentaenoic acid; EPA, eicosapentaenoic acid; HAP, haptophyta; OCH, ochrophyta; RHO, rhodophyta.

Species	Group	Strain	Palmitic $C_{16:0}$	Palmitoleic $C_{16:1}$ n-7	Stearic $C_{18:0}$	Oleic $C_{18:1}$ n-9	Linoleic $C_{18:2}$ n-6	Gamma-Linolenic $C_{18:3}$ n-6	Alpha-Linolenic $C_{18:3}$ n-3	Stearidonic $C_{18:4}$ n-3	Eicosenoic $C_{20:1}$ n-9	EPA $C_{20:5}$ n-3	DPA $C_{22:5}$ n-3	DHA $C_{22:6}$ n-3	References
Graesiella emersonii	CHL	GEGS21	27.5	-	0.6	22.2	26.3	1.0	22.1	-	0.3	-	-	-	This study
G. emersonii	CHL	CCAP 211/8P	19	1.6	2.3	53.8	4.8	6.7 *	-	-	-	-	-	-	[63]
G. emersonii	CHL	Maryland Culture Collection No. 2	28.3	2	-	31	5.9	17 *	-	2.1	-	-	-	-	[64]
G. emersonii	CHL	MAUA001	18.7	-	4.15	47.74	13.72	-	-	-	-	-	-	-	[40]
G. emersonii	CHL	MM0036	16.8	0.9	1.7	17.6	10.7	-	27.2	-	-	-	-	-	[28]
G. emersonii	CHL	NFW2	20.93	3.41	0.19	8.4	4.01	-	45.04	-	-	16.39	-	-	[65]
G. emersonii	CHL	NT1e	18.79	2.39	2.04	23.79	11.04	18.36	-	-	0.29	-	-	-	[66]
G. emersonii	CHL	SXND-25	14.8	6.5	3.2	44.5	10.1	12.9 *	-	-	-	-	-	-	[67]
Amphidinium carterae	DINO	UTEX LB 1002	30.9	7.1	10.5	0.3	5.6	3.1 *	-	-	-	15.1	1.3	17	[68]
Auxenochlorella protothecoides	CHL	MM0012	7.1	1	1.8	3.8	29.4	-	21.9	-	-	-	-	-	[28]
Chaetoceros affinis	BACI	B02	26	33.9	3.2	2.8	1.3	-	0.8	-	-	0.6	-	0.1	[69]
C. calcitrans	BACI	CS-I78	10.7	30	0.8	2.8	0.8	0.4	-	0.5	-	11.1	-	0.8	[70]
Chlamydomonas hedleyi	CHL	MM0020	18.3	2.6	1.2	-	9.8	-	16.4	-	-	-	-	-	[28]
C. oblonga	CHL	YSL07	40	-	2	3	37	2	16	-	-	-	-	-	[71]
Chlorella gloriosa	CHL	MM0063	22.5	0.4	1	2.2	10.6	-	-	-	-	-	-	-	[57]
C. minutissima	CHL	UTEX 2341	12.5	19.4	0.4	4.5	2.1	3.6 *	-	-	-	31.8	-	-	[72]
C. pyrenoidosa	CHL	SJTU-2	27.9	0.7	0.8	2.2	5.9	35.8 *	-	-	-	-	-	-	[73]
C. sorokiniana	CHL	MM0034	27.7	1.2	1.4	5.9	9.4	-	23.1	-	-	-	-	-	[28]
C. vulgaris	CHL	CCAP 211/8K	20.3	4.2	1.4	4.2	15.5	21.7 *	-	-	-	-	-	-	[63]
Coelastrum microporum	CHL	IBL-C119	25.66	1	2.91	44.24	8.58	11.12	-	-	-	-	-	-	[74]
Crypthecodinium cohnii	DINO	UTEX L1649	20.6	22.6	9	0.3	2.3	1.1 *	-	-	-	-	2	19.9	[68]
Dunaliella salina	CHL	LIMS-PS-1511	19.3	-	1.6	3.7	5.6	-	31.7	-	-	-	-	-	[28]
D. tertiolecta	CHL	CS-I75	14.7	0.1	0.4	2	4.8	2.7	43.5	1	-	-	-	-	[70]
Effrenium voratum	DINO	MABIKLP88	22.1	9.3	0.7	3.3	0.6	0.9	0.3	15.2	-	10.9	-	25.4	[75]
Haematococcus pluvialisa	CHL	-	22.49	0.64	3.15	19.36	20.23	0.86	16.18	-	0.13	0.57	-	-	[76]
Heterosigma akashiwo	OCH	Q01	44.8	16.1	0.5	1.6	1.6	-	4.1	7.1	-	8.4	-	0.7	[69]
Isochrysis galbana	HAP	SW2	23.18	32.13	-	.4.01	0.39	-	5.82	-	-	9.07	-	0.99	[65]
Jaagichlorella luteoviridis	CHL	MM0014	20.7	-	1.4	7.1	35.6	-	16.2	-	-	-	-	-	[77]
Microglena monadina	CHL	NFW3	25.09	3.28	0.4	-	14.47	-	53.01	-	-	-	-	-	[65]
Nannochloropsis oculata	OCH	CCAP 849/1	26.65	38.12	2.42	9.14	-	-	-	-	-	12.13	-	-	[78]
Phaeodactylum tricornutum	BACI	B24 A	22.3	32.7	1.7	1.5	4.1	0.2	2.8	0.2	-	12.5	-	0.8	[69]
Porphyridium purpureum	RHO	R01	42.5	-	1.4	1.4	2.5	0.2	6.6	0.9	-	8.3	-	0.1	[69]
Prorocentrum cordatum	DINO	S1	33.45	2.04	5.05	2.51	2.23	4.09	2.28	12.33	7.3	2.91	-	20.87	[79]
P. micans	DINO	D06	61.9	0.6	3.2	3.2	0.7	-	4.5	3.3	-	0.1	-	2.8	[69]
Schizochytrium aggregatum	BIG	ATCC 28209	15.3	18.6	8	14.7	15.1	0.6 *	-	-	-	15.7	-	-	[68]
Scrippsiella acuminata	DINO	D08	47.6	0.5	5.3	7.4	0.8	-	2	3.2	-	0.1	-	4.2	[69]
Skeletonema costatum	BACI	CS-181	16.5	28.6	0.8	1.4	2.2	0.3	0.3	2.2	-	6	-	2	[70]
Tetradesmus dimorphus	CHL	NT8c	22.21	1.9	1.59	24.45	6.29	17.71	-	-	0.33	-	-	-	[66]
T. obliquus	CHL	MM0026	18	2	1.3	16.4	5.2	-	28.3	-	-	-	-	-	[28]
Tetraedron caudatum	CHL	NT5	7.16	1.43	0.46	6.13	3.45	11.77	-	-	-	-	-	-	[66]

Table 6. *Cont.*

Species	Group	Strain	Individual Fatty Acids as Percentages of Total Fatty Acids													References
			Palmitic	Palmitoleic	Stearic	Oleic	Linoleic	Gamma-Linolenic	Alpha-Linolenic	Stearidonic	Eicosenoic	EPA	DPA	DHA	
			$C_{16:0}$	$C_{16:1}$ n-7	$C_{18:0}$	$C_{18:1}$ n-9	$C_{18:2}$ n-6	$C_{18:3}$ n-6	$C_{18:3}$ n-3	$C_{18:4}$ n-3	$C_{20:1}$ n-9	$C_{20:5}$ n-3	$C_{22:5}$ n-3	$C_{22:6}$ n-3	
Tetraselmis chuii	CHL	SW4	24.98	1.9	0.13	5.43	12.85	-	29.96	-	-	18.01	-	-	[65]
T. suecica	CHL	P03A	36.8	0.9	3	11.4	5	-	11.5	6.7	1.9	4.2	-	0.8	[69]
T. marina	CHL	P02D	28.8	3.8	2.1	6.2	1.6	0.2	16	8	-	5.8	-	-	[69]
Thalassiosira pseudonana	BACI	CS-173	11.2	18	0.7	0.5	0.4	0.2	0.1	5.3	0.2	19.3	-	3.9	[70]
Second-generation oil sources															
Jatropha	-	-	13.4	0.8	6.4	36.5	42.1	-	0.2	-	0.1	-	-	-	[80]
Karanja	-	-	7.4	-	3.8	65.6	15.4	4.4	-	-	-	-	-	-	[81]
Mahua	-	-	21.5	-	19	39.1	19.6	0.16	-	-	-	-	-	-	[82]
Palm	-	-	47.9	0.04	4.23	37	9.07	0.26	-	-	-	-	-	-	[83]
Rapeseed	-	-	3.49	-	0.85	64.4	22.3	8.23	-	-	-	-	-	-	[84]

* Not clear whether it is alpha-linolenic acid ($C_{18:3}$ n-3) or gamma-linolenic acid ($C_{18:3}$ n-6).

Biodiesel properties, including SV, IV, DU, MUFA, LCSF, CFPP, CN, and OS, based on FAME profiles were calculated using the biodiesel property equations [58]. As shown in Table 7, *G. emersonii* showed relatively higher IV (124.79) and PUFA (49.40), and lower CN (46.25), MUFA (22.50), LCSF (3.05), and OS values (4.98) compared to other plants and microalgae. However, *G. emersonii* GEGS21 showed relatively lower IV than those of *C. minutissima* UTEX 2341 and *Microglena monadina* NFW3, and higher CN values than those of *M. monadina* NFW3, respectively. The biodiesel standards EN14214 and ASTM D6751-02 establish the quality of biodiesel suitable for diesel engines. EN14214 and ASTM D6751-02 had slightly different biodiesel standards. Specifically, while a suitable standard IV was established lower than 120 and CN was higher than 51 in EN14214, the ASTM D6751-02 standard does not include IV as a standard specification. Moreover, ASTM D6751-02 suggests an upper limit for CN of 47, and a suitable standard OS was established above 6 and 3 in the EN14214 and ASTM D6751-02 standards, respectively.

Table 7. Biodiesel properties calculated from the FAME compositions of the isolated algal strain and other crops, and biodiesel standard EN 14214 and ASTMD6751-02. SV, saponification value; IV, iodine value; DU, degree of unsaturation; MUFA, monounsaturated fatty acid; PUFA, polyunsaturated fatty acid; LCSF, long-chain saturation factor; CFPP, cold filter plugging point; CN, cetane number; OS, oxidative stability.

Source	SV	IV	DU	MUFA	PUFA	LCSF	CFPP	CN	OS
Jatropha	190.98	105.42	122.10	37.30	42.40	4.54	−2.21	51.16	5.37
Karanja	184.05	94.22	105.20	65.60	19.80	2.64	−8.18	54.76	8.55
Mahua	191.58	67.72	78.62	39.10	19.76	11.65	20.12	59.55	8.56
Palm	194.82	48.05	55.70	37.04	9.33	6.91	5.22	63.50	15.23
Rapeseed	188.61	115.07	125.46	64.40	30.53	0.77	−14.05	49.35	6.45
Graesiella emersonii GEGS21	194.74	124.79	121.30	22.50	49.40	3.05	−6.89	46.25	4.98
Chlamydomonas hedleyi MM0020	95.60	62.09	55.00	2.60	26.20	2.43	−8.84	89.42	7.09
Chlorella gloriosa MM0063	132.19	100.26	85.00	2.60	41.20	2.75	−7.84	65.03	5.45
Chlorella minutissima UTEX 2341	142.74	162.79	98.90	23.90	37.50	1.45	−11.92	47.91	23.28
Coelastrum microporum IBL-C119	181.83	82.61	84.64	45.24	19.70	4.02	−3.84	57.73	8.58
Dunaliella salina LIMS-PS-1511	121.29	95.41	78.30	3.70	37.30	2.73	−7.90	69.83	5.75
Haematococcus pluvialisa	162.70	98.86	95.81	20.13	37.84	3.82	−4.46	57.60	5.75
Microglena monadina NFW3	188.54	166.15	138.24	3.28	67.48	2.71	−7.97	37.86	4.34
Jaagichlorella luteoviridis MM0014	157.60	109.69	110.70	7.10	51.80	2.77	−7.77	56.25	4.87
Tetradesmus obliquus MM0026	138.92	98.63	85.40	18.40	33.50	2.45	−8.78	63.40	6.11
EN14214	-	≤120	-	-	-	-	(≤−20~5)	≥51	≥6
ASTM D6751-02	-	-	-	-	-	-	-	≥47	≥3

3.5. Analysis of Microalgal Pigment Profile

The pigment profiles of *G. emersonii* GEGS21 are listed in Table 8. The pigment compositions of the isolate were chlorophyll *a* (19.1 mg g^{-1} DW), lutein (1.49 mg g^{-1} DW), neoxanthin (1.23 mg g^{-1} DW), chlorophyll *b* (Chl b, 0.85 mg g^{-1} DW), β-carotene (0.84 mg g^{-1} DW), zeaxanthin (0.46 mg g^{-1} DW), and α-carotene (0.16 mg g^{-1} DW). Other minor peaks were not identified owing to the lack of available commercial standard reagents.

Table 8. Photosynthetic pigment composition of isolated algal strain *Graesiella emersonii* GEGS21.

Pigments	Retention Time	Peak Area	Amount (mg g^{-1})
Neoxanthin	6.524	83.04	1.23
Unidentified	6.792	154.9	-
Lutein	10.654	152.39	1.49
Zeaxanthin	10.863	30.693	0.46
Chlorophyll *b*	14.215	23.784	0.85
Chlorophyll *a*	15.643	388.65	19.1
α-carotene	18.66	18.773	0.16
β-carotene	18.872	83.927	0.84

4. Discussion

Microalgal biomass has attracted increasing attention because it produces useful value-added compounds for bioenergy, cosmeceuticals, nutraceuticals, and pharmaceuticals via environmentally friendly bioprocesses [85]. Microalgae have a variety of advantages over other biodiesel feedstocks because they do not compete with food crops and exhibit faster growth rates that can result in considerably higher carbon sequestration rates than terrestrial plants. To investigate the potential bioenergy and other biotechnological applications, we identified and analyzed the biochemical properties of the indigenous algal isolate.

The genus *Graesiella* is a unicellular microalga comprising ellipsoidal and globose cells. The cell wall exhibited a meridional or irregular network of fine ribs on its surface. Ultrastructurally, the vegetative cells were uninuclear, single cup-shaped, and had parietal chloroplasts, each with one pyrenoid surrounded by starch plates. The cell wall was double-layered, with an inner polysaccharide and outer trilaminar. In this genus, asexual reproduction occurs through 2–16 autospores released via the rupture of the parental cell wall [34,60]. Morphological and physiological characteristics determined by light, fluorescence, and electron microscopy suggested that the isolate shared typical morphological and asexual reproduction characteristics with those of the genus *Graesiella* (Table 3). In addition, *G. emersonii* GEGS21 shared morphological characteristics with Maryland Culture Collection No. 2, CCMP421, and NIES-226 (Table 3). In particular, the morphological features of this isolate resembled those of strain NIES-226 as it had a single cup-shaped chloroplast, numerous vacuoles, more than two nuclei in mature cells, more than two daughter cells in parental cells, a pyrenoid matrix surrounded by starch grains, and a trilaminar sheath cell wall (Table 3). However, the cell wall of the strain NIES-226 does not always have meridional ribs on its surface [60], whereas most cells of the strain GEGS21 had meridional ribs (Figure 3a). It would be worthwhile to examine whether other *G. emersonii* strains have meridional ribs on the surface of most cells. The size of vegetative and daughter cells of the *G. emersonii* GEGS21 (8.79–14.4 μm and 5.0–12.7 μm, respectively) were similar to those of other strains of *G. emersonii* reported at 3.1–17.0 μm and 5.0–7.1 μm, respectively (Table 3).

The SSU rDNA sequence was also identical to that of the *G. emersonii* strains CCAP211/11N, BEA0616B, BEA1005B, NT1e, CCAP 211/15, CCAP 211/11M, CCAP 211/8H, and CCAP 211/8P (Table 4). Moreover, phylogenetic analysis confirmed that the strain GEGS21 is a member of *G. emersonii* (Figure 6). Based on the morphological and genetic results, this green alga was identified as *G. emersonii*.

Graesiella species have trilaminar sheaths, fibrillar walls, and plasma membranes in their cell walls [60,86]. *G. emersonii* GEGS21 shares these morphological characteristics. Afi et al. [63] reported the presence of a classical polysaccharide wall and a thin trilaminar outer wall composed of highly aliphatic, non-hydrolyzable macromolecules of *G. emersonii*. These polysaccharide walls are an important source for the paper, food, and textile industry, and for biofuel production as a by-product of biorefinery [87,88]. Thus, the cell wall of the GEGS21 strain can be used for biotechnological applications as a biorefinery by-product.

Prior to this study, *G. emersonii* strains were reported to inhabit mainly freshwater in Australia, China, Germany, Korea, India, Ireland, and Portugal [66,89–94]. In this study, many strains that inhabit freshwater were investigated (Figure 6, Table 4). However, the BEA1005B strain has been reported to inhabit brackish waters in Spain (GenBank accession

no. ON652615), and the strain MM0036 reported by Jo et al. [28] also inhabited brackish waters (27.2 PSU) in Korea. In this study, the strain GEGS21 was isolated from brackish water (21 PSU) in Korea. Strain CCAP211/11M was isolated from the soil (Figure 6). Therefore, *G. emersonii* is likely to be distributed in a variety of habitats, such as soil, freshwater, and brackish water, and this newly isolated GEGS21 strain could serve as a good example of a cosmopolite species found in different water environments. Indeed, *G. emersonii* showed the ability to grow in a range of salinities and was supported by physiological measurements taken on culture CCAP 211/11N, which showed that this strain grew optimally at ~2.5‰, but also grew at ~10‰ [62]. In addition, the maximal growth of *G. emersonii* GEGS21 was obtained at 0 M NaCl, but it also grew at ~0.5 M NaCl. The wide range of salinity tolerance may enable *G. emersonii* to survive in a wide variety of water environments around the world. Moreover, the salinity adaptability of *G. emersonii* GEGS21 facilitates large-scale cultivation, as it can be used as a growth medium in freshwater or seawater. Mandal and Chaurasia [92] reported that the lipid content of *G. emersonii* could be improved depending on the salt concentration added to the culture. In this report on salinity stress conditions, the maximum enhancement in lipid content (i.e., $58 \pm 2\%$ DCW) was obtained after 18 days incubation period under 0.3 M NaCl supplemented conditions [92]. Therefore, owing to the tolerance of *G. emersonii* GEGS21 to various salinity ranges, it can be used as a potential microalgal strain for commercial biodiesel production. In addition, *G. emersonii* GEGS21 could grow at temperatures of 5–40 °C; the highest growth rate was determined at 28–32 °C. The Indian *G. emersonii* strain can grow at temperatures ranging from 25–42 °C, with the highest growth observed at 38 °C [41,95]. It seems that the wide range of temperature tolerance of this species, related to *G. emersonii*'s survival and presence in a wide variety of water environments around the world, could facilitate large-scale cultivation under outdoor conditions. In conclusion, *G. emersonii* GEGS21 is easy to cultivate and can serve as a potential biological resource for various applications.

Analysis of the major cellular fatty acid composition of the strain GEGS21 revealed that it is rich in palmitic acid ($C_{16:0}$, 27.5%), oleic acid ($C_{18:1}$ n-9, 22.2%), linoleic acid ($C_{18:2}$ n-6, 26.3%), and α-linolenic acid ($C_{18:3}$ n-3, 22.1%) (Table 5). Previous studies have reported that palmitic acid could be used as an ideal competent source for biodiesel production owing to its high CN. In addition, it is used in pharmaceuticals, cosmetics, lube oils, water proofing, and food-grade additives [96,97]. Owing to these industrial uses, the global palmitic acid market was valued at USD 21.19 million in 2020 and predicted to have a 2.48% annual growth by 2027 [98].

The percentage of $C_{16:0}$ in *G. emersonii* GEGS21 (27.5%) was the highest among the reported *G. emersonii* strains, except for the *G. emersonii* strain Maryland Culture Collection No. 2 (28.3%) and was higher than that of the second-generation oil sources such as jatropha, karanja, mahua, and rapeseed (3.49–21.5%), except for palm (47.9%) (Table 6). In general, microalgae show higher photosynthetic efficiency and greater oil production than terrestrial plant sources [99]. Therefore, *G. emersonii* GEGS21 could be considered as a potential alternative plant source for biodiesel production. To compare the biodiesel quality of the isolated microalgae with that of terrestrial plants, the biodiesel properties were calculated based on the FAME profiles. It has been reported that the quality of biodiesel depends on FAME profiles [100,101]. Thereafter, the biodiesel quality parameters can be calculated from the FAME compositions, which provide information on the chain lengths and unsaturation, as shown in Table 7 [58]. In particular, several biodiesel properties, including IV, CN, and OS, are considered important for the application of diesel engines. The European standard EN14214 and American standard ASTM D6751-02 provide specific standard values for qualitative biodiesel. Compared with other terrestrial plants such as jatropha, karanja, palm, mahua, and rapeseed and microalgal strains including *Chlamydomonas hedleyi* MM0020, *Chlorella gloriosa* MM0063, *Coelastrum microporum* IBL-C119, *Dunaliella salina* LIMS-PS-1511, *Haematococcus pluvialisa*, *Jaagichlorella luteoviridis* MM0014, and *Tetradesmus obliquus* MM0026, *G. emersonii* GEGS21 had relatively higher IV and lower CN and OS values. However, *G. emersonii* GEGS21 represented lower IV than those of *Chlorella minutissima*

UTEX 2341 and *Microglena monadina* NFW3 and higher CN values than those of *M. monadina* NFW3, respectively. As shown in Table 7, whereas the established upper limits of IV and the lower limits of CN and OS are 120, 51, and 6 in EN14214, respectively, the lower limits of CN and OS in the ASTM D6751-02 biodiesel standard are 47 and 3, respectively. In this study, most terrestrial plants showed suitable IV, CN, and OS (Table 7). IV is defined as the amount of iodine (g) in a specific biodiesel and is related to the number of double bonds that affect the DU, OS, and cold flow of the biodiesel [58,100]. CN is an important parameter that reflects engine performance, the generation of nitrous oxide, and the combustion of biodiesel [58,100]. Although the biodiesel properties of the isolated alga *G. emersonii* showed a slightly higher value of IV (124.79) and a lower value of CN (46.25) than the standard values (IV: ≤ 120; CN: ≥ 47), it is expected that the biodiesel produced from *G. emersonii* can be used as a blending resource for the transportation of diesel fuels as an alternative energy source because biodiesel blends with fossil diesel have been widely offered as automotive fuels worldwide [102]. However, further studies are required to promote properties and quality of microalgal biodiesel by applying different cultivation techniques and using other biotechnological parameters because microalgal fatty acid profiles largely depend on nutritional status and multiple environmental factors such as temperature, light intensity, pH, substrate, and carbon and nitrogen ratio [103]. Additionally, numerous studies have shown that essential PUFAs have various beneficial health effects [104]. Moreover, signaling molecules that regulate inflammation, cardiac function, and tumor growth are biosynthesized by PUFAs [105–107]. These properties indicate the potential of PUFAs for nutraceutical and pharmaceutical purposes, and a variety of commercial products containing these PUFAs are available worldwide. Humans, like other mammals, are unable or poorly able to synthesize essential PUFAs, such as linoleic acid and α-linolenic acid. Therefore, direct uptake of these compounds from external sources is necessary. These sources include fish, mollusks, crustaceans, meat, milk, eggs, plants, and microalgae [108,109].

The percentage of omega-6 ($C_{18:2}$ n-6, 26.3%) of *G. emersonii* GEGS21 was the highest among the reported *G. emersonii* strains (4.0–22.0%) and was higher than that of other microalgae species (0.6–25.2%), except for the Chlorophyta *Chlamydomonas oblonga* YSL07 (37.0%), *Jaagichlorella luteoviridis* MM0014 (35.6%), and *Auxenochlorella protothecoides* MM0012 (29.4%) (Table 6). In addition, the percentage of omega-6 in *G. emersonii* GEGS21 was the highest among the second-generation oil plant sources, including karanja, palm, mahua, and rapeseed (9.07-22.3%), except for jatropha (42.1%) (Table 6). Omega-6 PUFAs are primarily derived from plant sources, such as sunflower, corn, and soybean oils, and a large number of commercial products are available worldwide. Therefore, this isolate has the potential to be used as an alternative to plant-based sustainable PUFA sources.

Pigment analysis revealed that the major carotenoids found in *G. emersonii* GEGS21 include the antioxidants neoxanthin and lutein (Table 8). The neoxanthin (1.23 mg g^{-1}) and lutein (1.49 mg g^{-1}) contents of *G. emersonii* GEGS21 were the highest among the reported *G. emersonii* strains (0.09-0.4 mg g^{-1}, neoxanthin; 0.56-1.34 mg g^{-1}, lutein) (Table 9). Lutein has certain beneficial pharmaceutical effects on human health owing to its strong ocular-protective, antioxidative, and anti-inflammatory properties [110,111]. Thus, the lutein market is growing rapidly, and the market size was worth about USD 288 million in 2020, predicted to have a 6.1% annual growth by 2027 [112]. Currently, potent commercial sources are mainly extracted from marigold flower petals [113], but the lutein content in marigold flowers is very low (0.3 mg g^{-1}), and the extraction process requires several steps which results in low yields. Compared with marigold, the concentration of lutein in microalgae is generally higher (>0.3 mg g^{-1}, Table 8). In addition, though lutein exists in green vegetables, some seeds (such as corn), and fruits, the content is low (up to ca. 0.4 mg g^{-1}) [111], and therefore they cannot be used as substitute materials for large-scale production. Improved productivity can be achieved by evaluating the effects of various culture conditions, including media components, on *G. emersonii* GEGS21 growth. Therefore, *G. emersonii* GEGS21 has the potential to be used as an alternative lutein source.

Table 9. Photosynthetic pigment composition comparisons of *Graesiella emersonii* strains and other microalgae. DCW: dry cell weight; NE: neoxanthin; VI: violaxanthin; AS: astaxanthin; MY: myxoxanthophyll; AN: antheraxanthin; LU: lutein; ZE: zeaxanthin; CA: canthaxanthin; EC: echinenone; AC: α-carotene; BC: β-carotene; CHA: chlorophyll a; CHB: chlorophyll b; FU: fucoxanthin; CHL: chlorophyte; BACI: bacillariophyte (diatom).

Species	Group	Strain	Pigment Composition in mg g^{-1} DCW														References
			NE	VI	AS	MY	AN	LU	ZE	CA	EC	AC	BC	CHA	CHB	FU	
Graesiella emersonii	CHL	GEGS21	1.23	-	-	-	-	1.49	0.46	-	-	0.16	0.84	19.1	0.85	-	This study
G. emersonii	CHL	CCNM1001	0.13	0.18	0.03	0	0	0.89	0.34	0.06	0	0	0.1	1.88	2.06	-	[114]
G. emersonii	CHL	CCNM 1011	0.09	0.08	0.03	0	0	0.56	0.17	0.13	0	0.01	0.08	0.97	1.18	-	[114]
G. emersonii	CHL	CCNM 1015	0.4	0.14	0.08	0	0	1.34	0.59	0.11	0	0.15	0.59	4.46	4.6	-	[114]
Botryococcus braunii	CHL	UTEX572	-	-	-	-	-	0.7	0.1	-	-	0.1	0.2	-	-	-	[115]
Bracteacoccus pseudominor	CHL	CCNM 1018	0.23	0.09	0	0	0	1.16	0.38	0	0	0.04	0.17	2.85	2.86	-	[114]
Chlorella minutissima	CHL	MCC-27	-	-	-	-	-	7.05	-	-	-	-	-	-	-	-	[116]
C. sorokiniana	CHL	FZU60	-	-	-	-	-	11.22	-	-	-	-	-	-	-	-	[117]
C. variabilis	CHL	CCNM 1017	0.3	0.08	0	0	0.07	1.13	0.36	0.03	0	0.04	0.17	2.4	2.43	-	[114]
C. vulgaris	CHL	UTEX 265	-	-	-	-	-	9.82	-	-	-	-	-	-	-	-	[118]
Desmodesmus subspicatus	CHL	CCNM 1008	2.73	0	0.37	0	0.07	1.98	0.23	0.04	0	0.04	0.26	6.6	7.21	-	[114]
Ettlia oleoabundans	CHL	UTEX 1185	-	-	-	-	-	3.4	0.1	0.5	-	0.6	0.6	-	-	-	[115]
Monoraphidium minutum	CHL	CCNM 1042	0.59	0.43	0.27	0	0.16	2.2	1.11	0.15	0	0.12	0.53	0.84	6.66	-	[114]
Phaeodactylum tricornutum	BACI	CCMP 1327	-	-	-	-	-	2.1	0.1	0.6	-	0.1	1.6	-	-	24.3	[115]
Tetradesmus dimorphus	CHL	CCNM 1045	4.13	0.02	0.07	0	0.02	2	0.54	0.06	0	0.1	0.32	2.37	10.79	-	[114]
T. obliquus	CHL	UTEX 2016	-	-	-	-	-	1.6	1.6	0.3	-	0.2	0.4	-	-	-	[115]

Several microalgae species have great potential to produce healthy food and feed supplements. *G. emersonii* is used as a raw food material in European countries, such as Austria, Germany, and Switzerland, and is authorized as a food supplement in France [42,43]. There are cases where it has been approved as a food additive, so it is more likely to be approved as a food or food additive in other countries in the future. Hence, the *G. emersonii* strain GEGS21 may have the potential to be used as a raw food material and aid future commercial applications in European countries.

In this study, we provided a record of *G. emersonii* in Korea based on morphological and molecular data. The accurate identification of the isolate was achieved using our findings. In addition, this microalga could serve as a promising candidate for further phylogenetic studies in research fields as well as a potential biological resource to produce biofuels and biochemicals of commercial interest in industrial fields.

Author Contributions: Conceptualization, N.S.K., K.C. and J.W.H.; methodology, N.S.K., S.M.A., H.K., C.H.L. and E.S.K.; software, N.S.K. and S.M.A.; validation, K.C., S.M.A. and G.C.; investigation, H.K. and K.C.; resources, E.S.K., H.K. and C.H.L.; data curation, N.S.K. and K.C.; writing—original draft preparation, N.S.K.; writing—review and editing, J.W.H.; visualization, N.S.K. and K.C.; supervision, J.W.H.; project administration, K.C.; funding acquisition, K.C. All authors have read and agreed to the published version of the manuscript.

Conflicts of Interest: The authors declare no conflict of interest.

References

1. Corliss, J.O. Biodiversity and biocomplexity of the protists and an overview of their significant roles in maintenance of our biosphere. *Acta Protozool.* **2002**, *41*, 199–219.
2. Huss, V.A.; Ciniglia, C.; Cennamo, P.; Cozzolino, S.; Pinto, G.; Pollio, A. Phylogenetic relationships and taxonomic position of *Chlorella*-like isolates from low pH environments (pH < 3.0). *BMC Evol. Biol.* **2002**, 2, 13.
3. Jeong, H.J.; Yoo, Y.D.; Kim, J.S.; Seong, K.A.; Kang, N.S.; Kim, T.H. Growth, feeding and ecological roles of the mixotrophic and heterotrophic dinoflagellates in marine planktonic food webs. *Ocean. Sci. J.* **2010**, *45*, 65–91. [CrossRef]
4. La Rocca, N.; Andreoli, C.; Giacometti, G.M.; Rascio, N.; Moro, I. Responses of the Antarctic microalga *Koliella antarctica* (Trebouxiophyceae, Chlorophyta) to cadmium contamination. *Photosynthetica* **2009**, *47*, 471–479. [CrossRef]
5. Metting, F.B. Biodiversity and application of microalgae. *J. Ind. Microbiol.* **1996**, *17*, 477–489. [CrossRef]
6. Little, S.M.; Senhorinho, G.N.A.; Saleh, M.; Basiliko, N.; Scott, J.A. Antibacterial compounds in green microalgae from extreme environments: A review. *Algae* **2021**, *36*, 61–72. [CrossRef]
7. Arrigo, K.R. Marine microorganisms and global nutrient cycles. *Nature* **2005**, *437*, 349–355. [CrossRef]
8. Cuellar-Bermudez, S.P.; Garcia-Perez, J.S.; Rittmann, B.E.; Parra-Saldivar, R. Photosynthetic bioenergy utilizing CO_2: An approach on flue gases utilization for third generation biofuels. *J. Clean. Prod.* **2015**, *98*, 53–65. [CrossRef]
9. Leu, S.; Boussiba, S. Advances in the production of high-value products by microalgae. *Ind. Biotechnol.* **2014**, *10*, 169–183. [CrossRef]
10. Tsukahara, K.; Sawayama, S. Liquid fuel production using microalgae. *J. Jpn. Pet. Inst.* **2005**, *48*, 251. [CrossRef]
11. Carrasco-Reinado, R.; Escobar, A.; Carrera, C.; Guarnizo, P.; Vallejo, R.A.; Fernández-Acero, F.J. Valorization of microalgae biomass as a potential source of high-value sugars and polyalcohols. *LWT* **2019**, *114*, 108385. [CrossRef]
12. Cezare-Gomes, E.A.; del Mejia-da-Silva, L.C.; Pérez-Mora, L.S.; Matsudo, M.C.; Ferreira-Camargo, L.S.; Singh, A.K.; de Carvalho, J.C.M. Potential of microalgae carotenoids for industrial application. *Appl. Biochem. Biotechnol.* **2019**, *188*, 602–634. [CrossRef]
13. de Oliveira, A.P.F.; Bragotto, A.P.A. Microalgae-based products: Food and public health. *Future Foods* **2022**, *6*, 100157. [CrossRef]
14. Hu, I.C. Production of potential coproducts from microalgae. In *Biofuels from Algae*; Lee, D.J., Pandey, A., Chang, J.-S., Chisti, Y., Soccol, C.R., Eds.; Elsevier: Amsterdam, The Netherlands, 2019; pp. 345–358.
15. Orejuela-Escobar, L.; Gualle, A.; Ochoa-Herrera, V.; Philippidis, G.P. Prospects of microalgae for biomaterial production and environmental applications at biorefineries. *Sustainability* **2021**, *13*, 3063. [CrossRef]
16. Chew, K.W.; Yap, J.Y.; Show, P.L.; Suan, N.H.; Juan, J.C.; Ling, T.C.; Lee, D.J.; Chang, J.S. Microalgae biorefinery: High value products perspectives. *Bioresour. Technol.* **2017**, *229*, 53–62. [CrossRef] [PubMed]

17. Olguín, E.J.; Sánchez-Galván, G.; Arias-Olguín, I.I.; Melo, F.J.; González-Portela, R.E.; Cruz, L.; De Philippis, R.; Adessi, A. Microalgae-based biorefineries: Challenges and future trends to produce carbohydrate enriched biomass, high-added value products and bioactive compounds. *Biology* **2022**, *11*, 1146. [CrossRef] [PubMed]

18. Pomeroy, B.; Grilc, M.; Likozar, B. Artificial neural networks for bio-based chemical production or biorefining: A review. *Renew. Sustain. Energ. Rev.* **2022**, *153*, 111748. [CrossRef]

19. Sivaramakrishnan, R.; Suresh, S.; Kanwal, S.; Ramadoss, G.; Ramprakash, B.; Incharoensakdi, A. Microalgal biorefinery concepts' developments for biofuel and bioproducts: Current perspective and bottlenecks. *Int. J. Mol. Sci.* **2022**, *2*, 2623. [CrossRef]

20. Srimongkol, P.; Sangtanoo, P.; Songserm, P.; Watsuntorn, W.; Karnchanatat, A. Microalgae-based wastewater treatment for developing economic and environmental sustainability: Current status and future prospects. *Front. Bioeng. Biotechnol.* **2022**, *10*, 904046. [CrossRef]

21. Šoštarič, M.; Klinar, D.; Bricelj, M.; Golob, J.; Berovič, M.; Likozar, B. Growth, lipid extraction and thermal degradation of the microalga *Chlorella vulgaris*. *New Biotechnol.* **2012**, *29*, 325–331. [CrossRef]

22. Eleršek, T.; Flisar, K.; Likozar, B.; Klemenčič, M.; Golob, J.; Kotnik, T.; Miklavčič, D. Electroporation as a solvent-free green technique for non-destructive extraction of proteins and lipids from *Chlorella vulgaris*. *Front. Bioeng. Biotechnol.* **2020**, *8*, 443. [CrossRef] [PubMed]

23. Kumar, V.; Al Momin, S.; Kumar, V.V.; Ahmed, J.; Al-Musallam, L.; Shajan, A.B.; Al-Aqeel, H.; Al-Zakri, W.M. Distribution and diversity of eukaryotic microalgae in Kuwait waters assessed using 18S rRNA gene sequencing. *PLoS ONE* **2021**, *16*, e0250645. [CrossRef] [PubMed]

24. Leliaert, F.; Tronholm, A.; Lemieux, C.; Turmel, M.; DePriest, M.S.; Bhattacharya, D.; Karol, K.G.; Fredericq, S.; Zechman, F.W.; Lopez-Bautista, J.M. Chloroplast phylogenomic analyses reveal the deepest-branching lineage of the chlorophyta, Palmophyllophyceae Class. *Nov. Sci. Rep.* **2016**, *6*, 25367. [CrossRef] [PubMed]

25. Stanković, N.; Kostić, I.; Jovanović, B.; Savić-Zdravković, S.; Matić, S.; Bašić, J.; Cvetković, T.; Simeunović, J.; Milošević, D. Can phytoplankton blooming be harmful to benthic organisms? The toxic influence of *Anabaena* sp. and *Chlorella* sp. on *Chironomus riparius* larvae. *Sci. Total Environ.* **2020**, *729*, 138666. [CrossRef]

26. Hong, J.W.; Kang, N.S.; Jang, H.S.; Kim, H.J.; An, Y.R.; Yoon, M.; Kim, H.S. Biotechnological potential of Korean marine microalgal strains and its future prospectives. *Ocean Polar Res.* **2019**, *41*, 289–309.

27. Hong, J.W.; Kim, O.H.; Jo, S.-W.; Kim, H.; Jeong, M.R.; Park, K.M.; Lee, K.I.; Yoon, H.-S. Biochemical composition of a Korean domestic microalga *Chlorella vulgaris* KNUA027. *Microbiol. Biotechnol. Lett.* **2016**, *44*, 400–407. [CrossRef]

28. Jo, S.W.; Kang, N.S.; Lee, J.A.; Kim, E.S.; Kim, K.M.; Yoon, M.; Hong, J.W.; Yoon, H.S. Characterization of MABIK microalgae with biotechnological potentials. *J. Mar. Biosci. Biotechnol.* **2020**, *12*, 40–49.

29. Pulz, O.; Gross, W. Valuable products from biotechnology of microalgae. *Appl. Microb. Biotechnol.* **2004**, *65*, 635–648. [CrossRef]

30. Champenois, J.; Marfaing, H.; Pierre, R. Review of the taxonomic revision of *Chlorella* and consequences for its food uses in Europe. *J. Appl. Phycol.* **2015**, *27*, 1845–1851. [CrossRef]

31. Borowitzka, M. Systematics, taxonomy and species names: Do they matter? In *The Physiology of Microalgae*; Developments in Applied Phycology; Borowitzka, M.A., Beardall, J., Raven, J.A., Eds.; Springer International Publishing: Dordrecht, The Netherlands, 2016; pp. 655–681.

32. Gantar, M.; Svircev, Z. Microalgae and cyanobacteria: Food for thought. *J. Phycol.* **2008**, *44*, 260–268. [CrossRef]

33. Vardaka, E.; Kormas, K.A.; Katsiapi, M.; Genitsaris, S.; Moustaka-Gouni, M. Molecular diversity of bacteria in commercially available "*Spirulina*" food supplements. *Peer J.* **2016**, *4*, e1610. [CrossRef] [PubMed]

34. Kalina, T.; Puncochárová, M. Taxonomy of the subfamily Scotiellocystoideae Fott 1976 (Chlorellaceae, Chlorophyceae). *Arch. Hydrobiol. Suppl. Algol. Stud.* **1987**, *45*, 473–521.

35. Guiry, M.D.; Guiry, G.M. *AlgaeBase. World-Wide Electronic Publication*; National University of Ireland Galway: Galway, Ireland, 2022. Available online: http://www.algaebase.org (accessed on 18 October 2022).

36. Robinson, P.K. Immobilized algal technology for wastewater treatment purposes. In *Wastewater Treatment with Algae*; Wong, Y.S., Tam, N.F.Y., Eds.; Springer-Verlag & Landes Bioscience: Berlin, Germany, 1998; pp. 1–16.

37. Xu, M.; Bernards, M.; Hu, Z. Algae-facilitated chemical phosphorus removal during high-density *Chlorella emersonii* cultivation in a membrane bioreactor. *Bioresour. Technol.* **2014**, *153*, 383–387. [CrossRef] [PubMed]

38. Desai, S.S.; Singh, R.D.; Ghosh, S.B.; Kelkar, V. A novel strategy for disarming quorum sensing in *Pseudomonas aeruginosa-Chlorella emersonii* KJ725233. *J. Appl. Biol. Biotechnol.* **2020**, *8*, 78–83.

39. Kumar, V.S.; das Sarkar, S.; Das, B.K.; Sarkar, D.J.; Gogoi, P.; Maurye, P.; Mitra, T.; Talukder, A.K.; Ganguly, S.; Nag, S.K. Sustainable Biodiesel Production from Microalgae *Graesiella emersonii* through Valorization of Garden Wastes-Based Vermicompost. *Sci. Total Environ.* **2022**, *807*, 150995. [CrossRef] [PubMed]

40. Perdana, B.A.; Dharma, A.; Zakaria, I.J.; Syafrizayanti, S. Freshwater pond microalgae for biofuel: Strain isolation, identification, cultivation and fatty acid content. *Biodiversitas* **2021**, *22*, 505–511. [CrossRef]

41. Sawant, S.S.; Mane, V.K. Nutritional profile, antioxidant, antimicrobial potential, and bioactives profile of *Chlorella emersonii* KJ725233. *Asian J. Pharm. Clin. Res.* **2018**, *11*, 220–225. [CrossRef]

42. Araújo, R.; Peteiro, C. *Algae as Food and Food Supplements in Europe. EUR 30779 EN.*; Publications Office of the European Union: Luxembourg, 2021. Available online: https://publications.jrc.ec.europa.eu/repository/handle/JRC125913 (accessed on 16 October 2022).

43. Mendes, M.C.; Navalho, S.; Ferreira, A.; Paulino, C.; Figueiredo, D.; Silva, D.; Gao, F.; Gama, F.; Bombo, G.; Jacinto, R.; et al. Algae as food in Europe: An overview of species diversity and their application. *Foods* **2022**, *11*, 1871. [CrossRef]

44. Grama, B.S.; Chader, S.; Khelifi, D.; Agathos, S.N.; Jeffryes, C. Induction of canthaxanthin production in a *Dactylococcus* microalga isolated from the Algerian Sahara. *Bioresour. Technol.* **2014**, *151*, 297–305. [CrossRef]

45. Granéli, E.; Flynn, K. Chemical and physical factors influencing toxin content. In *Ecology of Harmful Algae*; Granéli, E., Turner, J.T., Eds.; Springer: Berlin/Heidelberg, Germany, 2006; Volume 189, pp. 229–241.

46. Huelsenbeck, J.P.; Ronquist, F. MrBayes: Bayesian inference of phylogeny. *Bioinformatics* **2001**, *17*, 754–755. [CrossRef]

47. Ronquist, F.; Huelsenbeck, J.P. MRBAYES 3: Bayesian phylogenetic inference under mixed models. *Bioinformatics* **2003**, *19*, 1572–1574. [CrossRef] [PubMed]

48. Kang, N.S.; Jeong, H.J.; Moestrup, Ø.; Shin, W.G.; Nam, S.W.; Park, J.Y.; de Salas, M.F.; Kim, K.W.; Noh, J.H. Description of a new planktonic mixotrophic dinoflagellate *Paragymnodinium shiwhaense* n. gen., n. sp. from the coastal waters off western Korea: Morphology, pigments, and ribosomal DNA gene sequence. *J. Eukaryot. Microbiol.* **2010**, *57*, 121–144. [CrossRef]

49. Stamatakis, A. RAxML version 8: A tool for phylogenetic analysis and post-analysis of large phylogenies. *Bioinformatics* **2014**, *30*, 1312–1313. [CrossRef] [PubMed]

50. Medlin, L.; Elwood, H.J.; Stickel, S.; Sogin, M.L. The characterization of enzymatically amplified eukaryotic 16S-like rRNA-coding regions. *Gene* **1988**, *71*, 491–499. [CrossRef]

51. Litaker, R.W.; Vandersea, M.W.; Kibler, S.R.; Reece, K.S.; Stokes, N.A.; Steidinger, K.A.; Millie, D.F.; Bendis, B.J.; Pigg, R.J.; Tester, P.A. Identification of *Pfiesteria piscicida* (Dinophyceae) and *Pfiesteria*-like organisms using internal transcribed spacers-specific PCR assays. *J. Phycol.* **2003**, *39*, 754–761. [CrossRef]

52. Weekers, P.; Gast, R.J.; Fuerst, P.A.; Byers, T.J. Sequence variations in small-subunit ribosomal RNAs of *Hartmannella vermiformis* and their phylogenetic implications. *Mol. Biol. Evol.* **1994**, *11*, 684–690.

53. Scholin, C.A.; Herzog, M.; Sogin, M.; Anderson, D.M. Identification of group and strain specific genetic makers for globally distributed *Alexandrium* (Dinophyceae) II. Sequence analysis of a fragment of the LSU rRNA gene. *J. Phycol.* **1994**, *30*, 999–1011. [CrossRef]

54. Hadi, S.I.I.A.; Santana, H.; Brunale, P.P.M.; Gomes, T.G. DNA barcoding green microalgae isolated from neotropical inland waters. *PLoS ONE* **2016**, *11*, e0149284. [CrossRef]

55. Heo, J.; Cho, D.H.; Ramanan, R.; Oh, H.M.; Kim, H.S. PhotoBiobox: A tablet sized, low-cost, high throughput photobioreactor for microalgal screening and culture optimization for growth, lipid content and CO_2 sequestration. *Biochem. Eng. J.* **2015**, *103*, 193–197. [CrossRef]

56. Breuer, G.; Evers, W.A.C.; de Vree, J.H.; Kleinegris, D.M.M.; Martens, D.E.; Wijffels, R.H.; Lamers, P.P. Analysis of fatty acid content and composition in microalgae. *J. Vis. Exp.* **2013**, *80*, e50628. [CrossRef]

57. Kang, N.S.; Lee, J.A.; Jang, H.S.; Kim, K.M.; Kim, E.S.; Yoon, M.; Hong, J.W. First record of a marine microalgal species, *Chlorella gloriosa* (Trebouxiophyceae) isolated from the Dokdo Islands, Korea. *Korean J. Environ. Biol.* **2019**, *37*, 526–534. [CrossRef]

58. Islam, M.A.; Magnusson, M.; Brown, R.J.; Ayoko, G.A.; Nabi, M.N.; Heimann, K. Microalgal species selection for biodiesel production based on fuel properties derived from fatty acid profiles. *Energies* **2013**, *6*, 5676–5702. [CrossRef]

59. Baek, K.L.; Yu, J.; Jeong, J.; Sim, S.J.; Bae, S.; Jin, E.S. Photoautotrophic production of macular pigment in a *Chlamydomonas reinhardtii* strain generated by using DNA-free CRISPR-Cas9 RNP-mediated mutagenesis. *Biotechnol. Bioeng.* **2018**, *115*, 719–728. [CrossRef] [PubMed]

60. Nozaki, H.; Katagiri, M.; Nakagawa, M.; Aizawa, K.; Watanabe, M.M. Taxonomic re-examination of two strains labeled 'Chlorella' in the microbial culture collection at the National Institute for Environmental Studies (NIES-Collection). *Microbiol. Cult. Collect.* **1995**, *11*, 11–18.

61. Shihira, I.; Krauss, R.W. *Chlorella, Physiology and Taxonomy of Forty-One Isolates*; No. NASA-CR-69107; University of Maryland: College Park, MD, USA, 1965.

62. Bark, M. Cultivation of Eleven Different Species of Freshwater Microalgae using Simulated Flue Gas Mimicking Effluents from Paper Mills as Carbon Source. Master's Thesis, Chalmers University of Technology, Gothenburg, Sweden, 2012.

63. Afi, L.; Metzger, P.; Largeau, C.; Connan, J.; Berkaloff, C.; Rousseau, B. Bacterial degradation of green microalgae: Incubation of *Chlorella emersonii* and *Chlorella vulgaris* with *Pseudomonas oleovorans* and *Flavobacterium aquatile*. *Org. Geochem.* **1996**, *25*, 117–130. [CrossRef]

64. Frasinel, C.; Patterson, G.W.; Dutky, S.R. Effect of triarimol on sterol and fatty acid composition of three species of *Chlorella*. *Phytochemistry* **1978**, *17*, 1567–1570. [CrossRef]

65. Andrew, A.R.; Yong, W.T.L.; Misson, M.; Anton, A.; Chin, G.J.W.L. Selection of tropical microalgae species for mass production based on lipid and fatty acid profiles. *Front. Energy Res.* **2022**, *10*, 912904. [CrossRef]

66. Duong, V.T.; Ahmed, F.; Thomas-hall, S.R.; Quigley, S.; Nowak, E.; Schenk, P.M. High protein- and high lipid-producing microalgae from northern Australia as potential feedstock for animal feed and biodiesel. Front. *Bioeng. Biotechnol.* **2015**, *3*, 53.

67. Cheng, W.; Shao, X.; Song, C.; Shi, F.; Ji, C.; Li, R. Effects of nitrogen stress on growth and oil accumulation of *Chlorella emersonii*. *Biotechnol. Bull.* **2017**, *33*, 160–165.

68. Vazhappilly, R.; Chen, F. Eicosapentaenoic acid and docosahexaenoic acid production potential of microalgae and their heterotrophic growth. *J. Am. Oil Chem. Soc.* **1998**, *75*, 393–397. [CrossRef]

69. Viso, A.C.; Marty, J.C. Fatty acids from 28 marine microalgae. *Phytochemistry* **1993**, *34*, 1521–1533. [CrossRef]

70. Volkman, J.K.; Jeffrey, S.W.; Nichols, P.D.; Rogers, G.I.; Garland, C.D. Fatty acid and lipid composition of 10 species of microalgae used in mariculture. *J. Exp. Mar. Biol. Ecol.* **1989**, *128*, 219–240. [CrossRef]

71. Salama, E.-S.; Kim, H.-C.; Abou-Shanab, R.I.; Ji, M.-K.; Oh, Y.-K.; Kim, S.-H.; Jeon, B.-H. Biomass, lipid content, and fatty acid composition of freshwater *Chlamydomonas mexicana* and *Scenedesmus obliquus* grown under salt stress. *Bioprocess Biosyst. Eng.* **2013**, *36*, 827–833. [CrossRef]

72. Vanderploeg, H.A.; Liebig, J.R.; Gluck, A.A. Evaluation of different phytoplankton for supporting development of zebra mussel larvae (*Dreissena polymorpha*): The importance of size and polyunsaturated fatty acid content. *J. Great Lakes Res.* **1996**, *22*, 36–45. [CrossRef]

73. Tang, D.; Han, W.; Li, P.; Miao, X.; Zhong, J. CO_2 biofixation and fatty acid composition of *Scenedesmus obliquus* and *Chlorella pyrenoidosa* in response to different CO_2 levels. *Bioresour. Technol.* **2011**, *102*, 3071–3076. [CrossRef]

74. Nascimento, I.A.; Marques, S.S.I.; Cabanelas, I.T.D.; Pereira, S.A.; Druzian, J.I.; de Souza, C.O.; Vich, D.V.; de Carvalho, G.C.; Nascimento, M.A. Screening microalgae strains for biodiesel production: Lipid productivity and estimation of fuel quality based on fatty acids profiles as selective criteria. *Bioenergy Res.* **2013**, *6*, 1–13. [CrossRef]

75. Kang, N.S.; Kim, E.S.; Lee, J.A.; Kim, K.M.; Kwak, M.S.; Yoon, M.; Hong, J.W. First report of the dinoflagellate genus *Effrenium* in the east sea of Korea: Morphological, genetic, and fatty acid characteristics. *Sustainability* **2020**, *12*, 3928. [CrossRef]

76. Damiani, M.C.; Popovich, C.A.; Constenla, D.; Leonardi, P.I. Lipid analysis in *Haematococcus pluvialis* to assess its potential use as a biodiesel feedstock. *Bioresour. Technol.* **2010**, *101*, 3801–3807. [CrossRef]

77. Kim, K.M.; Kang, N.S.; Jang, H.S.; Park, J.S.; Jeon, B.H.; Hong, J.W. Characterization of *Heterochlorella luteoviridis* (Trebouxiaceae, Trebouxiophyceae) isolated from the Port of Jeongja in Ulsan, Korea. *J. Mar. Biosci. Biotechnol.* **2017**, *9*, 22–29.

78. Tonon, T.; Harvey, D.; Larson, T.R.; Graham, I.A. Long-chain polyunsaturated fatty acid production and partitioning to triacyl-glycerols in four microalgae. *Phytochemistry* **2002**, *61*, 15–24. [CrossRef]

79. Makri, A.; Bellou, S.; Birkou, M.; Papatrehas, K.; Dolapsakis, N.P.; Bokas, D.; Papanikolaou, S.; Aggelis, G. Lipid synthesized by micro-algae grown in laboratory- and industrial-scale bioreactors. *Eng. Life Sci.* **2011**, *11*, 52–58. [CrossRef]

80. Becker, K.; Makkar, H.P.S. *Jatropha curcas*: A potential source for tomorrow's oil and biodiesel. *Lipid Technol.* **2008**, *20*, 104–107. [CrossRef]

81. Goembira, F.; Saka, S. Advanced supercritical methyl acetate method for biodiesel production from *Pongamia pinnata* oil. *Renew. Energy* **2015**, *83*, 1245–1249. [CrossRef]

82. Saravanan, N.; Nagarajan, G.; Puhan, S. Experimental investigation on a DI diesel engine fuelled with *Madhuca Indica* ester and diesel blend. *Biomass Bioenergy* **2010**, *34*, 838–843. [CrossRef]

83. Crabbe, E.; Nolasco-Hipolito, C.; Kobayashi, G.; Sonomoto, K.; Ishizaki, A. Biodiesel production from crude palm oil and evaluation of butanol extraction and fuel properties. *Process Biochem.* **2001**, *37*, 65–71. [CrossRef]

84. Ramadhas, A.S.; Muraleedharan, C.; Jayaraj, S. Performance and emission evaluation of a diesel engine fueled with methyl esters of rubber seed oil. *Renew. Energy* **2005**, *30*, 1789–1800. [CrossRef]

85. Odjadjare, E.C.; Mutanda, T.; Olaniran, A.O. Potential biotechnological application of microalgae: A critical review. *Crit. Rev. Biotechnol.* **2017**, *37*, 37–52. [CrossRef]

86. Allard, B.; Rager, M.N.; Templier, J. Occurrence of high molecular weight lipids (C_{80+}) in the trilaminar outer cell walls of some freshwater microalgae. A reappraisal of algaenan structure. *Org. Geochem.* **2002**, *33*, 789–801. [CrossRef]

87. Baudelet, P.; Ricochon, G.; Linder, M.; Muniglia, L. A new insight into cell walls of Chlorophyta. *Algal Res.* **2017**, *25*, 333–371. [CrossRef]

88. Kim, D.Y.; Vijayan, D.; Praveenkumar, R.; Han, J.I.; Lee, K.; Park, J.Y.; Chang, W.S.; Lee, J.S.; Oh, Y.K. Cell-wall disruption and lipid/astaxanthin extraction from microalgae: *Chlorella* and *Haematococcus*. *Bioresour. Technol.* **2016**, *199*, 300–310. [CrossRef]

89. Borkenstein, C.G.; Knoblechner, J.; Frühwirth, H.; Schagerl, M. Cultivation of *Chlorella emersonii* with flue gas derived from a cement plant. *J. Appl. Phycol.* **2011**, *23*, 131–135. [CrossRef]

90. Kim, M.J.; Shim, C.K.; Kim, Y.K.; Hong, S.J.; Park, J.H.; Han, E.J.; Ji, H.J.; Yoon, J.C.; Kim, S.C. Isolation and morphological identification of fresh water green algae from organic farming habitats in Korea. *Korean J. Org. Agric.* **2014**, *22*, 743–760. [CrossRef]

91. Malis, S.A.; Cohen, E.; Ben Amotz, A. Accumulation of canthaxanthin in *Chlorella emersonii*. *Physiol. Plant.* **1993**, *87*, 232–236. [CrossRef]

92. Mandal, M.K.; Chaurasia, N. De novo transcriptomic analysis of *Graesiella emersonii* NC-M1 reveals differential genes expression in cell proliferation and lipid production under glucose and salt supplemented condition. *Renew. Energy* **2021**, *179*, 2004–2015. [CrossRef]

93. Wilson, M.; Houghton, J.A. Continuous cultivation of *Chlorella emersonii* on pig manure. *Ir. J. Agric. Res.* **1977**, *16*, 21–33.

94. Zhang, J.J.; Duan, L.L.; Cheng, W.L.; Ji, C.L.; Cui, H.L.; Li, R.Z. Algae-bacteria symbiosis increases biomass and oil production of *Chlorella emersonii*. *Biotechnol. Bull.* **2019**, *35*, 76–84. (In Chinese)

95. Sawant, S.S.; Joshi, A.A.; Bhagwat, A.; Mane, V.K. Tapping the antioxidant potential of a novel isolate *Chlorella emersonii*. *World J. Pharm. Res.* **2014**, *3*, 726–739.

96. Afifudeen, C.L.W.; Loh, S.H.; Aziz, A.; Takahashi, K.; Effendy, A.W.M.; Cha, T.S. Double-high in palmitic and oleic acids accumulation in a non-model green microalga, *Messastrum gracile* SE-MC4 under nitrate-repletion and -starvation cultivations. *Sci. Rep.* **2021**, *11*, 381. [CrossRef]

97. Priya, D.; Patil, A.; Niranjana, S.; Chavan, A. Potential testing of fatty acids from mangrove *Aegiceras corniculatum* (L.) Blanco. *Int. J. Pharm. Sci.* **2012**, *3*, 569–571.
98. Market Growth Reports. Global Palmitic Acid Market Report 2016–2027 by Companies, Regions, Types and Application. 2021. Available online: https://www.marketgrowthreports.com/global-palmitic-acid-market-19119624. (accessed on 30 September 2022).
99. Li, Y.; Horsman, M.; Wu, N.; Lan, C.Q.; Dubois-Calero, N. Biofuels from microalgae. *Biotech. Prog.* **2008**, *24*, 815–820. [CrossRef]
100. Cho, K.; Heo, J.; Cho, D.-H.; Tran, Q.-G.; Yun, J.-H.; Lee, S.-M.; Lee, Y.J.; Kim, H.-S. Enhancing algal biomass and lipid production by phycospheric bacterial volatiles and possible growth enhancing factor. *Algal Res.* **2019**, *37*, 186–194. [CrossRef]
101. Yilancioglu, K.; Cokol, M.; Pastirmaci, I.; Erman, B.; Cetiner, S. Oxidative stress is a mediator for increased lipid accumulation in a newly isolated *Dunaliella salina* strain. *PLoS ONE* **2014**, *9*, e91957. [CrossRef] [PubMed]
102. Kousoulidou, M.; Fontaras, G.; Ntziachristos, L.; Samaras, Z. Biodiesel blend effects on common-rail diesel combustion and emissions. *Fuel* **2010**, *89*, 3442–3449. [CrossRef]
103. El-Sayed, A.E.K.B.; Fetyan, N.A.; Moghanm, F.S.; Elbagory, M.; Ibrahim, F.M.; Sadik, M.W.; Shokr, M.S. Biomass fatty acid profile and fuel property prediction of bagasse waste grown *Nannochloropsis oculata*. *Agriculture* **2022**, *12*, 1201. [CrossRef]
104. Mehta, L.R.; Dworkin, R.H.; Schwid, S.R. Polyunsaturated fatty acids and their potential therapeutic role in multiple sclerosis. *Nat. Clin. Pract. Neurol.* **2009**, *5*, 82–92. [CrossRef]
105. Pereira, H.; Barreira, L.; Figueiredo, F.; Custódio, L.; Vizetto-Duarte, C.; Polo, C.; Rešek, E.; Engelen, A.; Varela, J. Polyunsaturated fatty acids of marine macroalgae: Potential for nutritional and pharmaceutical applications. *Mar. Drugs* **2012**, *10*, 1920–1935. [CrossRef]
106. Radwan, S.S. Sources of C_{20}-polyunsaturated fatty acids for biotechnological use. *Appl. Microbiol. Biot.* **1991**, *35*, 421–430. [CrossRef]
107. Vrablik, T.L.; Watts, J.L. Polyunsaturated fatty acid derived signaling in reproduction and development: Insights from *Caenorhabditis elegans* and *Drosophila melanogaster*. *Mol. Reprod. Dev.* **2013**, *80*, 244–259. [CrossRef]
108. Abedi, E.; Sahari, M.A. Long-chain polyunsaturated fatty acid sources and evaluation of their nutritional and functional properties. *Food Sci. Nutr.* **2014**, *2*, 443–463. [CrossRef]
109. Santin, A.; Russo, M.T.; Ferrante, M.I.; Balzano, S.; Orefice, I.; Sardo, A. Highly valuable polyunsaturated fatty acids from microalgae: Strategies to improve their yields and their potential exploitation in aquaculture. *Molecules* **2021**, *26*, 7697. [CrossRef]
110. Guerin, M.; Huntley, M.E.; Olaizola, M. *Haematococcus* astaxanthin: Applications for human health and nutrition. *Trends Biotechnol.* **2003**, *21*, 210–216. [CrossRef]
111. Zheng, H.; Wang, Y.; Li, S.; Nagarajan, D.; Varjani, S.; Lee, D.J.; Chang, J.S. Recent advances in lutein production from microalgae. *Renew. Sustain. Energy Rev.* **2022**, *153*, 111795. [CrossRef]
112. Maximize Market Research PVT. LTD. Global lutein Market Industry Analysis and Forecast (2021–2027)-by Form, by Source, by Production Process, by Application and Region. 2020. Available online: https://www.maximizemarketresearch.com/market-report/lutein-market/661/ (accessed on 30 September 2022).
113. Breithaupt, D.E.; Wirt, U.; Bamedi, A. Differentiation between lutein monoester regioisomers and detection of lutein diesters from marigold flowers (*Tagetes erecta*, L.) and several fruits by liquid chromatography-mass spectrometry. *J. Agric. Food Chem.* **2002**, *50*, 66–70. [CrossRef]
114. Paliwal, C.; Ghosh, T.; George, B.; Pancha, I.; Maurya, R.; Chokshi, K.; Ghosh, A.; Mishra, S. Microalgal carotenoids: Potential nutraceutical compounds with chemotaxonomic importance. *Algal Res.* **2016**, *15*, 24–31. [CrossRef]
115. Banskota, A.H.; Sperker, S.; Stefanova, R.; McGinn, P.J.; O'Leary, S.J.B. Antioxidant properties and lipid composition of selected microalgae. *J. Appl. Phycol.* **2018**, *31*, 309–318. [CrossRef]
116. Dineshkumar, R.; Subramanian, G.; Dash, S.K.; Sen, R. Development of an optimal light-feeding strategy coupled with semicontinuous reactor operation for simultaneous improvement of microalgal photosynthetic efficiency, lutein production and CO_2 sequestration. *Biochem. Eng. J.* **2016**, *113*, 47–56. [CrossRef]
117. Ma, R.; Zhang, Z.; Ho, S.-H.; Ruan, C.; Li, J.; Xie, Y.; Shi, X.; Liu, L.; Chen, J. Two-stage bioprocess for hyper-production of lutein from microalga *Chlorella sorokiniana* FZU60: Effects of temperature, light intensity, and operation strategies. *Algal Res.* **2020**, *52*, 102119. [CrossRef]
118. Gong, M.; Bassi, A. Investigation of *Chlorella vulgaris* UTEX 265 cultivation under light and low temperature stressed conditions for lutein production in flasks and the coiled tree photo-bioreactor (CTPBR). *Appl. Biochem. Biotechnol.* **2017**, *183*, 652–671. [CrossRef] [PubMed]